Journal of Chromatography B, 877 (2009) 3442–3455

Contents lists available at ScienceDirect

Journal of Chromatography B

journal homepage: www.elsevier.com/locate/chromb

GC–MS analysis of *S*-nitrosothiols after conversion to *S*-nitroso-*N*-acetyl cysteine ethyl ester and in-injector nitrosation of ethyl acetate☆

Dimitrios Tsikas[a,*], Sabine Dehnert[a], Karin Urban[a], Andrzej Surdacki[a], Hartmut H. Meyer[b]

[a] *Institute of Clinical Pharmacology, Hannover Medical School, Carl-Neuberg-Strasse 1, 30625 Hannover, Germany*
[b] *Institute of Organic Chemistry, Leibniz University Hannover Hannover, Germany*

ARTICLE INFO

Article history:
Received 30 March 2009
Accepted 23 June 2009
Available online 30 June 2009

Keywords:
N-Acetyl cysteine ethyl ester (NACET)
In-injector derivatization
Nitric oxide (NO)
S-Nitrosothiols
Stable isotopes
Thiols (RSH)
S-Transnitrosation

ABSTRACT

S-Nitrosothiols from low-molecular-mass and high-molecular-mass thiols, including glutathione, albumin and hemoglobin, are endogenous potent vasodilators and inhibitors of platelet aggregation. By utilizing the *S*-transnitrosation reaction and by using the lipophilic (pK_L 0.78) and strong nucleophilic synthetic thiol *N*-acetyl cysteine ethyl ester (NACET) we have developed a GC–MS method for the analysis of *S*-nitrosothiols and their ^{15}N- or ^{2}H–^{15}N-labelled analogs as *S*-nitroso-*N*-acetyl cysteine ethyl ester (SNACET) and S^{15}NACET or d_3-S^{15}NACET derivatives, respectively, after their extraction with ethyl acetate. Injection of ethyl acetate solutions of *S*-nitrosothiols produced two main reaction products, compound X and compound Y, within the injector in dependence on its temperature. Quantification was performed by selected-ion monitoring of *m/z* 46 (i.e., $[NO_2]^-$) for SNACET and *m/z* 47 (i.e., $[^{15}NO_2]^-$) for S^{15}NACET/d_3-S^{15}NACET for compound X, and *m/z* 157 for SNACET and *m/z* 160 for d_3-S^{15}NACET for compound Y. In this article we describe the development, validation and in vitro and in vivo applications of the method to aqueous buffered solutions, human and rabbit plasma. Given the ester functionality of SNACET/S^{15}NACET/d_3-S^{15}NACET, stability studies were performed using metal chelators and esterase inhibitors. The method was found to be suitable for the quantitative determination of various *S*-nitrosothiols including SNACET externally added to human plasma (0–10 μM). Nitrite contamination in ethyl acetate was found to interfere. Our results suggest that the concentration of endogenous *S*-nitrosothiols in human plasma does not exceed about 200 nM in total. Oral administration of S^{15}NACET to rabbits (40–63 μmol/kg body weight) resulted in formation of ALB-S^{15}NO, [^{15}N]nitrite and [^{15}N]nitrate in plasma.

1. Introduction

The reaction of sulfhydryl (SH) groups of thiols (RSH) with nitrosyl (NO^+) moieties-containing species, as they potentially occur in nitrous acid (HONO; see Eq. (1)), and its anhydride N_2O_3 (NO_2–NO), leads to formation of the corresponding thioesters, the *S*-nitrosothiols (R–S–N=O, RSNO). The most abundant thiol in human organism is L-cysteine (CysSH). Cysteine occurs in biological fluids and tissues both as the soluble amino acid and as a moiety in low-molecular-mass (LMM) thiols, such as the tripeptide glutathione (GSH), and in high-molecular-mass (HMM) proteins, such as human serum albumin (ALB-SH) and hemoglobin (Hb-SH) [1,2]. *S*-Nitrosoalbumin (ALB-SNO) and *S*-nitrosohemoglobin (Hb-SNO) belong to the most abundant endogenous *S*-nitrosothiols in human blood, whereas the LMM *S*-nitrosothiols of GSH and CysSH, i.e., GSNO and CysSNO, respectively, are hardly detectable in human blood even when using very sensitive analytical methods [3–9]. *S*-Nitrosothiols – in this work the term *S*-nitrosothiol is used in place of *S*-nitroso-cysteinyl thiols – exert potently many biological actions including vasodilation, inhibition of platelet aggregation, neurotransmission and cell signaling. These actions can be mediated both by cGMP-dependent and cGMP-independent mechanisms, for instance by releasing nitric oxide (NO) or by nitr(osyl)ating SH groups [10] which are widely known as *S*-transnitr(osyl)ation reactions [11,12]. Thus, the release of NO and the *S*-transnitrosation reaction between R_1SNO and R_2SH to form R_1SH and R_2SNO (see Eq. (2)) are the most important currently known chemical properties of *S*-nitrosothiols.

The analysis of *S*-nitrosothiols in biological samples is associated with many pre-analytical and analytical difficulties [8,9]. Methodological problems mainly arise from the lability of the *S*-nitroso group, the analytically challenging low concentrations of LMM and HMM *S*-nitrosothiols, their readily and abundant artifactual formation under acidic conditions, as well as from the need for

☆ This paper is part of the special issue "Analysis of Thiols", I. Dalle-Donne and R. Rossi (Guest Editors).

* Corresponding author. Tel.: +49 511 532 3959; fax: +49 511 532 2750.
E-mail address: tsikas.dimitros@mh-hannover.de (D. Tsikas).

1570-0232/$ – see front matter © 2009 Elsevier B.V. All rights reserved.
doi:10.1016/j.jchromb.2009.06.032

indirect detection in the majority of the currently available analytical methods for *S*-nitrosothiols [8,9]. As a result of these difficulties, reported plasma concentrations for endogenous *S*-nitrosothiols, notably ALB-SNO, Hb-SNO, GSNO and CysSNO, cover almost five orders of magnitude, e.g., between 0.3 nM for GSNO [13] and more than 10 μM for ALB-SNO [8]. For a thorough and critical discussion and comparison of currently available analytical methods for *S*-nitrosothiols see the review by Giustarini et al. [8].

Our group has shown that *S*-nitrosothiols, including ALB-SNO in human plasma [14,15], and GSNO and CysSNO in buffered solutions and treated erythrocytes [16], can be accurately determined by GC–MS after their conversion to nitrite and its subsequent derivatization to the pentafluorobenzyl derivatives. Specific analysis of *S*-nitrosothiols by GC–MS requires preceding separation of individual *S*-nitrosothiols, for instance by affinity column chromatography [14,15] or by HPLC [16]. Our GC–MS methods suggest that ALB-SNO is the most abundant HMM *S*-nitrosothiol in human plasma—the concentration of ALB-SNO in plasma of healthy humans in the basal state is about 160 nM, whereas the concentration of the LMM *S*-nitrosothiols GSNO and CysSNO is expected to be clearly below 10 nM [14,15].

Because of the controversy concerning *S*-nitrosothiol plasma concentrations in healthy humans [8,9], and given the unique feature of quantitative measurement by using stable-isotope labelled analogs as internal standards [17,18], we wanted to develop alternative GC–MS methods by means of which the concentration of *S*-nitrosothiols present in human plasma and in red blood cells could be determined in total. We tried to realize this by collectively converting plasma RSNO into *S*-nitroso-*N*-acetyl cysteine ethyl ester (SNACET) via *S*-transnitrosation reaction by means of the synthetic thiol *N*-acetyl cysteine ethyl ester (NACET), according to Eq. (3). It is noteworthy that SNACET is extractable into water-immiscible organic solvents such as ethyl acetate and chloroform because of its high lipophilicity and does not require additional derivatization for GC–MS analysis, unlike the free acid *S*-nitroso-*N*-acetyl cysteine (SNAC) [19]. In the present work we describe the development of new GC–MS methods and show their principal applicability to measure various *S*-nitrosothiols in human plasma in vitro and in vivo in plasma of rabbits orally administered with S^{15}NACET. The results of the present methods confirm previous findings from our group and many other groups and suggest that the concentration of *S*-nitrosothiols in plasma of healthy subjects in the basal state does not exceed about 200 nM in total.

$$R\text{–}S\text{–}H + HO\text{–}N{=}O \longleftrightarrow R\text{–}S\text{–}N{=}O + HO\text{–}H \quad (1)$$

$$R_2\text{–}S\text{–}H + R_1\text{–}S\text{–}N{=}O \longleftrightarrow R_2\text{–}S\text{–}N{=}O + R_1\text{–}S\text{–}H \quad (2)$$

$$NACET + RSNO \longleftrightarrow SNACET + RSH \quad (3)$$

2. Experimental

2.1. Materials and chemicals

Glutathione, *N*-ethylmaleimide (NEM), L-cysteine ethyl ester, acetic anhydride, 4-hydroxy-2,2,6,6-tetramethylpiperidin-1-oxyl (4-OH-TEMPO), 2,3,4,5,6-pentafluorobenzyl bromide, 2-fluorobenzyl bromide, 2,3,4,5,6-pentafluorobenzyl alcohol, 2,3,4,5,6-pentafluorobenzoyl chloride and [*acetyl*-$^2H_6$]acetic anhydride (declared as 99 at.% ^2H) were purchased from Sigma–Aldrich (Steinheim, Germany). Methanol of gradient grade and ethanol were supplied by Mallinckrodt Baker (Griesheim, Germany). Sodium nitrite was purchased from Riedel de Haën (Seelze, Germany). Sodium [^{15}N]nitrite (declared as 98 at.% ^{15}N) was purchased from Cambridge Isotope Laboratories (Andover, MA, USA). Glutathione (GSH), L-cysteine and *N*-acetyl-L-cysteine (NAC) were purchased from Sigma (Munich, Germany). Toluene, ethyl acetate and $HgCl_2$ were obtained from Merck (Darmstadt, Germany). HiTrapBlue Sepharose affinity columns (1- and 5-ml cartridges) for affinity column chromatography of ALB-SNO and ALB-S^{15}NO were obtained from Pharmacia Biotech (Freiburg, Germany). ALB-SNO and ALB-S^{15}NO standards were prepared by incubating albumin extracted from freshly obtained human plasma with unlabelled and ^{15}N-labelled butyl nitrite, respectively, and were isolated, characterized and standardized by GC–MS as described previously [20]. Unlabelled and ^{15}N-labelled LMM *S*-nitrosothiols were prepared by mixing equimolar solutions in distilled water of the corresponding thiol and unlabelled or ^{15}N-labelled nitrite and by acidifying with HCl (at a final HCl concentration of 50 mM) as described elsewhere [12], and were stored in an ice bath in the dark (i.e., aluminum foil) until immediate use. The structure of the LMM *S*-nitrosothiols prepared by this method was elucidated previously by ESI-MS [21]. Assuming stoichiometric and quantitative reaction [12,21], LMM *S*-nitrosothiol concentration in stock solutions was considered to be 4.8 mM. Phenylmethanesulfonyl fluoride (PMSF), diethylenetriaminepentaacetic acid (DTPA) and esterase (specific activity, 142 units/mg) were from FLUKA (Neu Ulm, Germany).

2.2. Synthesis of N-acetyl cysteine ethyl ester

N-Acetyl cysteine ethyl ester (NACET; $C_7H_{13}NO_3S$, MW 191.2) and [*acetyl*-$^2H_3$]-NACET (d_3-NACET; $C_7H_{10}{}^2H_3NO_3S$, MW 194.2) were prepared under argon atmosphere by *N*-acetylation of L-cysteine ethyl ester in dichloromethane with equimolar amounts of acetic anhydride and [*acetyl*-$^2H_6$]acetic anhydride, respectively, and purified by column chromatography. NACET (mp 44.1–44.5 °C) was structurally identified by electron ionization MS {70 eV; *m*/*z* (intensity, %): 74 (32), 76 (100), 86 (28), 99 (10), 102 (79), 118 (36), 132 (16), 146 (7), and 191 (23) M^+}, ^{1}H NMR {200 MHz, $CDCl_3$; δ (ppm): 1.32 (t, 7 Hz; CH_3), 1.34 (t, 9 Hz; SH), 2.07 (s, CH_3CO), 3.03 (dd, 9 Hz, 4 Hz; CH_2–S), 4.26 (m, CH_2), 4.87 (7 Hz, 4 Hz; CHN) and 6.45 (bs, NH)}, infrared spectrometry {chloroform; ν (cm^{-1}): 3428, 3000, 2940, 2908, 1736, 1676, 1504, 1444, 1420, 1376, 1340, 1312, 1200, 1136, 1096, 1036, 980, 860, 512}, and polarimetry ($[\alpha]_D^{25}$ = 61.55°; *c* = 2.64 in chloroform). Elemental analysis gave: 43.91% C (cal. 43.96%), 6.83% H (cal. 6.85%), and 7.26% N (cal. 7.32%). HPLC–UV (215 nm) analysis of NACET and d_3-NACET revealed a chemical purity of >99% for each compound.

2.3. GC–MS conditions

A Hewlett-Packard MS engine 5890 connected directly to a gas chromatograph 5890 series II equipped with an autosampler (sample tray capacity for 100 vials) Hewlett-Packard model 7673 (Waldbronn, Germany) was used for GC–MS analyses. GC–MS analyses were also performed on a GC–MS instrument model DSQ equipped with a gas chromatograph Focus GS and an autosampler (sample tray capacity for 105 vials) all from ThermoFisher (Dreieich, Germany). The gas chromatographs were equipped with fused-silica capillary columns Optima 17 (30 m × 0.25 mm i.d., 0.25-μm film thickness) from Macherey-Nagel (Düren, Germany). Aliquots (routinely 1 μl) of ethyl acetate extracts and other solvents were injected in the splitless mode by means of the autosamplers. The following oven temperature program was used with helium (50 kPa) as the carrier gas: 1 min at 40 °C, then increased to 280 °C at a rate of 30 °C/min. Interface, injector and ion source were kept at 260 °C, 250 °C (or as indicated in the respective experiments) and 180 °C, respectively, in both GC–MS apparatus. Electron energy and electron current were set to 200 eV and 300 μA, respectively. Negative-ion chemical ionization (NICI) with methane (200 Pa) as the reagent gas was used in quantitative analyses. Routinely, electron multiplier voltage was set to 1.8 kV. Quantification by GC–MS in the NICI mode was performed by selected-ion monitoring (SIM)

of selected ions using a dwell-time of 50 ms for each ion as specified in the respective experiments.

2.4. Biological samples—withdrawal of blood and generation of plasma

Approval from the local Ethics Committee of the Medical School of Hannover was obtained for studies in which blood from healthy male and female volunteers (aged 23–38 years) was taken for in vitro studies on human plasma. Blood was drawn from the antecubital vein using 9 ml EDTA-containing monovettes (Sarstedt, Germany). Immediately after collection, the blood was put in an ice bath. Plasma was prepared by centrifugation (10 min, 4 °C, 800 × *g*), pooled, portioned in 1-ml fractions and stored at −80 °C. In quantitative analyses plasma samples were used from only once thawed samples. Freshly prepared plasma samples and thawed plasma samples were stored in an ice bath and in the dark until analysis.

2.5. Procedures for the quantification of S-nitrosoalbumin

To 400-μl aliquots of plasma samples ALB-S^{15}NO was added to achieve a final concentration of 1 μM. Extraction of plasma albumin was performed on 1-ml HiTrapBlue Sepharose affinity columns preconditioned with 2 ml of buffer A (50 mM KH_2PO_4, pH 7.0 adjusted with 5 M NaOH). Cartridges were washed with 4 ml of buffer A, proteins were eluted with 2 ml of buffer B (50 mM KH_2PO_4, 1.5 M KCl, pH 7.0 adjusted with 5 M NaOH), and eluates were ultrafiltered by centrifugation up to a protein fraction volume of about 400 μl. Aliquots (100 μl) of the eluates or of the protein fraction of ultrafiltered samples were treated with 10-μl aliquots of a 10 mM aqueous solution of $HgCl_2$ and incubated for 1 h at room temperature to produce nitrite (i.e., [^{14}N]nitrite and [^{15}N]nitrite). These samples were analyzed for nitrite by GC–MS after derivatization with pentafluorobenzyl bromide as described [22]. In addition, 100-μl aliquots of non-ultrafiltered and ultrafiltered eluates were spiked with 10-μl aliquots of a 1 mM solution of NACET in buffer B. After incubation for 5 min at room temperature samples were extracted with ethyl acetate (1 ml) by vortex-mixing for 1 min. The ethyl acetate phase was decanted and dried over anhydrous Na_2SO_4. Prior to GC–MS analysis pentafluorobenzyl alcohol (dissolved in ethyl acetate) was added to the ethyl acetate phase at a final concentration of 1 mM.

2.6. Development, validation and in vitro applications of the method

For the sake of simplicity, the individual experiments, including those to method development, optimization and validation performed in the present work, are described in detail in the respective sections of Section 3. If not otherwise specified, all procedures including centrifugation were performed in the cold (0–8 °C) and with pre-cooled chemicals and solvents. Direct exposure to daylight was avoided where possible. Data are reported as mean ± standard deviation.

2.7. Oral administration of S^{15}NACET to the rabbit

In a pilot study we investigated the applicability of the method in vivo in the rabbit. This study was approved by the local supervisory Committee for Studies in Animals (Hannover, Germany). Chinchilla bastard rabbits from Charles River Deutschland were used (aged 3–4 months). Freshly prepared S^{15}NACET (280 nmol in 58 μl) was diluted in 1 mM glucose (1942 μl). An aliquot of 1.7 ml containing 238 nmol S^{15}NACET was administered orally by means of a 2-ml syringe to a 3.8-kg weighing male rabbit, corresponding to a dose of 62.6 nmol S^{15}NACET per kg body weight (bw). Before and at various times (4 min, 20 min, 30 min, 60 min, 120 min, 180 min, and 240 min) after administration, venous blood (about 3 ml, EDTA) was taken and plasma was generated immediately. Blood (0.5 ml) and blood plasma were extracted immediately with 1 ml of ethyl acetate each. After phase separation and drying the ethyl acetate phase over anhydrous Na_2SO_4 samples were analyzed by SIM of *m*/*z* 46 and *m*/*z* 47. In addition, plasma (0.4 ml) was analyzed for ALB-S^{15}NO as described previously [14]. [^{15}N]Nitrite and [^{15}N]nitrate were determined simultaneously in 0.1-ml aliquots of plasma by GC–MS as described previously [22] before and after incubation with 1 mM $HgCl_2$ for 60 min at room temperature. After performance and evaluation of this experiment, two other rabbits received orally 40.3 and 44.6 nmol S^{15}NACET/kg bw, and [^{15}N]nitrite and [^{15}N]nitrate were measured in plasma from blood taken 60 min after administration.

3. Results

3.1. GC–MS of NACET and SNACET in ethyl acetate in the absence of additives

Freshly prepared solutions of NACET, d_3-NACET, SNACET and d_3-SNACET in ethyl acetate were analyzed by GC–MS in the EI and NICI mode. In the EI mode, NACET and d_3-NACET eluted as single peaks at retention time (t_R) of about 6.6 min. Under the same GC and EI conditions, SNACET and d_3-SNACET also emerged from the column as single peaks at a t_R of about 5.2 min. The EI mass spectra obtained from these peaks are summarized in Table 1. Molecular cations were observed from NACET (*m*/*z* 191) and d_3-NACET (*m*/*z* 194) but not from SNACET and d_3-SNACET, suggesting that the *S*-nitroso groups of SNACET and d_3-SNACET are thermally labile. The appearance of *m*/*z* 157 (from SNACET) and *m*/*z* 160 (from d_3-SNACET) are indicative of the loss of thionitrous acid (HSNO, 63 Da) from these molecules during GC–MS analysis.

Analysis of the same samples of SNACET and d_3-SNACET under the same GC–MS conditions except for NICI revealed several peaks of which the major peak eluted at about t_R 5.2 min. The most intense anions in the NICI mass spectra of these SNACET and d_3-SNACET peaks were *m*/*z* 157 and *m*/*z* 160. At a t_R of about 3.3 min a compound eluted with a single ion in its NICI mass spectrum at *m*/*z* 46 due to nitrite ($[NO_2]^-$) both from SNACET and from d_3-SNACET. The NICI mass spectra of the [^{15}N-*nitroso*]-labelled SNACET (i.e., S^{15}NACET) and [^{15}N-*nitroso*]-labelled d_3-SNACET (i.e., d_3-S^{15}NACET) also contained a single ion at *m*/*z* 47 due to $[^{15}NO_2]^-$. These findings suggest that under the GC–MS conditions used SNACET degrades thermally to produce two major products which emerge from the GC column at t_R 3.3 min and 5.2 min (Fig. 1). In the following, the substances eluting at t_R 3.3 min and 5.2 min are referred to as compound X and compound Y, respectively.

By analyzing a 2 mM solution of d_3-S^{15}NACET in ethyl acetate we investigated by SIM of *m*/*z* 47 and *m*/*z* 160 the effect of the injector temperature on the formation of compound X and compound Y. Fig. 2 shows that the injector temperature has great and distinctly different effects on the formation of these compounds. At an injector temperature of 150 °C, both compounds are virtually absent. The peak area of compound X increased sharply by increasing the injector temperature from 200 °C to 250 °C, but it decreased also sharply by increasing the injector temperature from 300 °C to 350 °C. The peak area of compound Y increased constantly with increasing injector temperature in a sigmoid fashion (Fig. 2). The peak area ratio (PAR) of *m*/*z* 160 to *m*/*z* 47 was 2.7:1 at 250 °C and 7.6:1 at 300 °C. We decided to set the injector temperature at 250 °C at which the peak areas of both compounds were closer.

Table 1
Major ions present in the GC–MS electron ionization mass spectra of NACET, d_3-NACET, SNACET and d_3-SNACET[a].

NACET *m/z* (%)	Ion assignment	d_3-NACET *m/z* (%)	Ion assignment
43 (84)	$[CH_3CO]^+$	46 (84)	$[CD_3CO]^+$
60 (100)	$[CH_3CONH_3]^+$	63 (100)	$[CD_3CONH_3]^+$
76 (44)	$[M-CH_3CH_2OCO-CH_2CO]^+$	77 (44)	$[M_{(d3)}-CH_3CH_2OCO-CD_2CO]^+$
102 (28)	$[NH_2-CH-COOCH_2CH_3]^+$	103 (26)	$[NHD-CH-COOCH_2CH_3]^+$
118 (11)	$[M-CH_3CH_2OCO]^+$	121 (10)	$[M_{(d3)}-CH_3CH_2OCO]^+$
132 (5)	$[M-CH_3CONH_2]^+$	132 (5)	$[M_{(d3)}-CD_3CONH_2]^+$
146 (2)	$[M-CH_3CH_2O]^+$	149 (2)	$[M_{(d3)}-CH_3CH_2O]^+$
191 (3)	$[M]^+$	194 (2)	$[M_{(d3)}]^+$
SNACET *m/z* (%)	Ion assignment	d_3-SNACET *m/z* (%)	Ion assignment
43 (100)	$[CH_3CO]^+$	46 (100)	$[CD_3CO]^+$
71 (16)	$[NH_2-C(=CH_2)-CHO]^+$	72 (22)	$[NHD-C(=CH_2)-CHO]^+$
87 (5)	$[NH_2-C(=CH_2)-COOCH_2CH_3]^+$	88 (5)	$[NHD-C(=CH_2)-OOCH_2CH_3]^+$
111 (11)	Not assigned	114 (19)	Not assigned
115 (17)	$[M-HSNO-CH_2=CO]^+$	116 (22)	$[M_{(d3)}-HSNO-CD_2=CO]^+$
157 (17)	$[M-HSNO]^+$	160 (26)	$[M_{(d3)}-HSNO]^+$
220 (0)	$[M]^+$	223 (0)	$[M_{(d3)}]^+$

M and $M_{(d3)}$ are the molecular masses of the unlabelled and ^2H-labelled compounds, respectively. The GC retention time was 5.152 min for d_3-SNACET, 5.168 min for SNACET, 6.608 min for d_3-NACET, and 6.626 min for NACET. The HP instrument was used; the injector temperature was 250 °C.

[a] 500 pmol of each compound from 1 mM solutions in ethyl acetate were injected.

3.1.1. Analysis of SNACET in ethyl acetate solution

The results reported above suggested that SNACET could be quantitatively analyzed by GC–MS by using S^{15}NACET or d_3-S^{15}NACET as internal standard (IS). To test this we analyzed in duplicate solutions of SNACET in ethyl acetate of varying concentration (0 μM, 10 μM, 20 μM, 40 μM, 60 μM, 80 μM and 100 μM) using d_3-S^{15}NACET as IS at a fixed concentration of 100 μM and SIM of *m/z* 46 and *m/z* 47 for compound X and *m/z* 157 and *m/z* 160 for compound Y. The concentration of the analyte (A) SNACET in its solutions (C_A) was calculated by multiplying the PAR of *m/z*

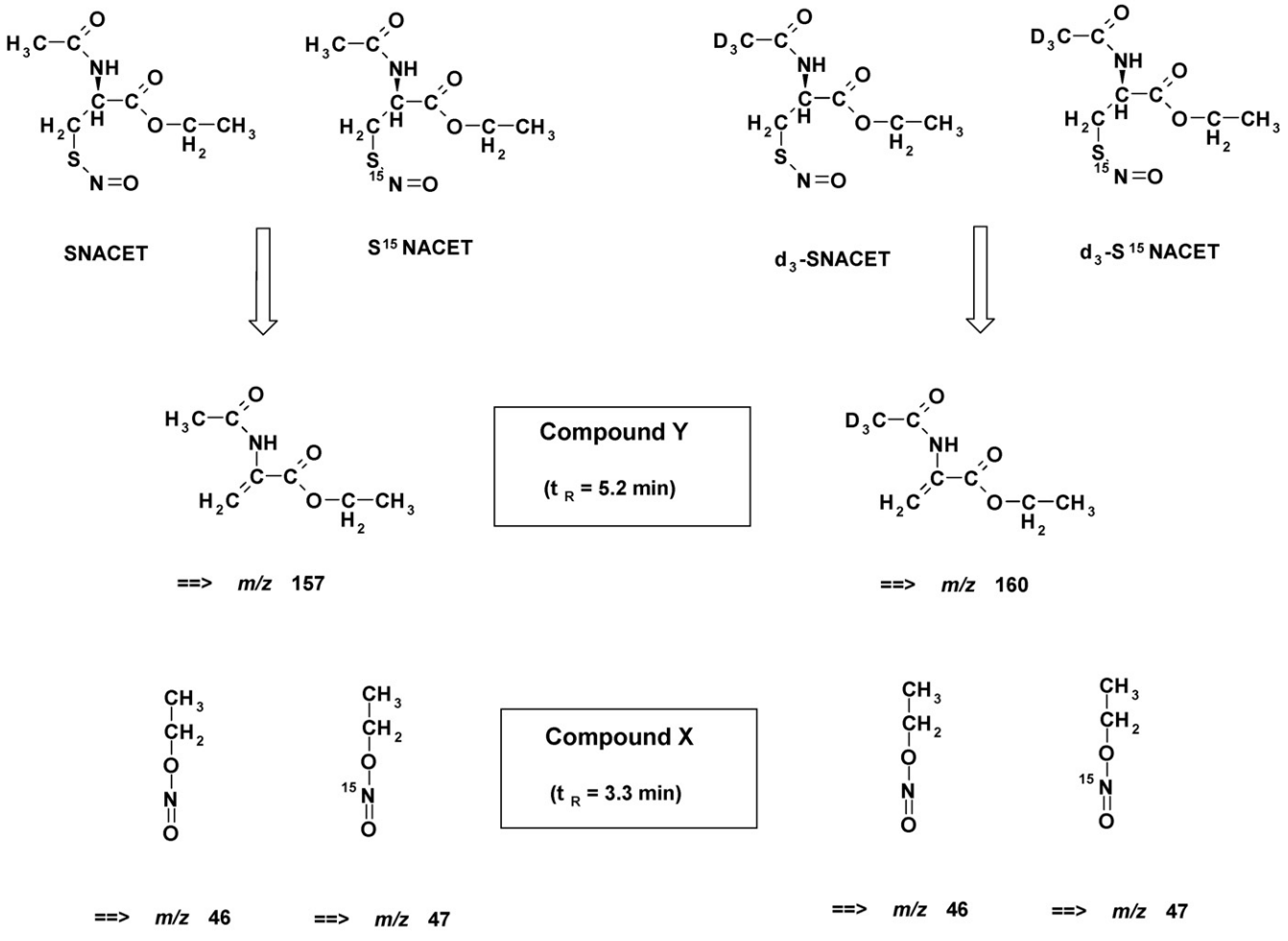

Fig. 1. Chemical structures of SNACET, S^{15}NACET, d_3-SNACET and d_3-S^{15}NACET and proposed structures for the SNACET-derived species eluting at 3.3 min and ionizing to *m/z* 46 and *m/z* 47 (compound X), and eluting at 5.2 min and ionizing to *m/z* 157 and *m/z* 160 (compound Y).

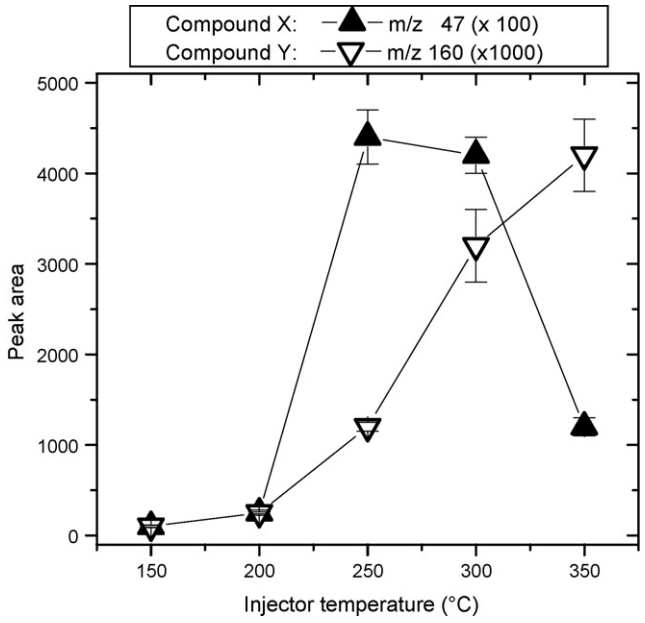

Fig. 2. Effect of the injector temperature on the area of the peaks eluting at 3.3 min (*m*/*z* 47) and 5.2 min (*m*/*z* 160). Each 500 pmol of d_3-S^{15}NACET (2 mM in ethyl acetate) were injected in duplicate at the indicated injector temperatures (starting at 150 °C) and selected-ion monitoring of *m*/*z* 47 and *m*/*z* 160 was performed in the NICI mode. Note the different magnification for the peak area. The HP GC–MS instrument was used.

46 to *m*/*z* 47 for compound X ($PAR_{46/47}$) and the PAR of *m*/*z* 157 to *m*/*z* 160 for compound Y ($PAR_{157/160}$) by the concentration of the IS (C_{IS}) according to the formula: $C = PAR \times C_{IS}$. Linear regression analysis between measured SNACET concentration (y) and added SNACET concentration (x) revealed the regression equations: $y_1 = 0.36 + 1.07x_1$ ($r_1 = 0.996$) for compound X and $y_2 = 0.41 + 0.94x_2$ ($r_2 = 0.996$) for compound Y. The slopes of the regression equations, being close to unity (slope ratio, 1.14:1), indicate almost complete recovery of SNACET and prove the principal utility of this method for quantitative determination of SNACET by GC–MS by detecting compound X and/or compound Y.

3.1.2. Analysis of SNACET in aqueous solutions

3.1.2.1. Analysis of SNACET in aqueous solutions without external addition of nitrite. We tested the applicability of the method for aqueous buffered solutions of SNACET in the concentration range of 0–10 μM using d_3-S^{15}NACET as the IS at a final added concentration of 10 μM. Thus, 1-ml solutions of SNACET in 0.1 M Tris buffer, pH 7.4 (adjusted by 5 M HCl), were spiked with the IS and extracted by vortex-mixing with ethyl acetate (1 ml) for 30 s. After centrifugation, the ethyl acetate phase was decanted, dried over anhydrous Na_2SO_4 and analyzed by GC–MS. Linear regression analysis between measured (y) and added (x) SNACET concentrations resulted in the regression equations: $y_1 = 0.34 + 0.86x_1$ ($r_1 = 0.9999$) for compound X and $y_2 = 0.195 + 0.92x_2$ ($r_2 = 0.992$) for compound Y, with the slope ratio being 0.94:1.

3.1.2.2. Analysis of SNACET in ethyl acetate and in aqueous solution with external addition of nitrite. Regularly, SNACET-containing ethyl acetate solutions should not contain inorganic nitrite and nitrate. However, this may not always be completely avoided because ethyl acetate and water are not entirely immiscible and because SNACET may decompose to nitrite and/or nitrate in its ethyl acetate solutions during storage. To investigate a potential interference of nitrite with SNACET analysis by GC–MS we performed two series of experiments in duplicate for each nitrite concentration examined. In experiment A, 10-μl aliquots of aqueous solutions of nitrite (i.e., $[^{14}N]$nitrite or $[^{15}N]$nitrite) were added under vortex-mixing to 1-ml aliquots of an ethyl acetate solution of SNACET and S^{15}NACET (each at 250 nM) to achieve final added $[^{14}N]$nitrite or $[^{15}N]$nitrite concentrations of up to 100 μM for each anion in the ethyl acetate solution. In experiment B, a solution of SNACET and S^{15}NACET (each at 250 nM) was prepared in 0.2 M Tris buffer, pH 7.4. To 1-ml aliquots of these solutions, aqueous solutions of $[^{14}N]$nitrite or $[^{15}N]$nitrite were added to achieve final added concentrations of up to 100 μM for each anion. These samples were extracted by vortex-mixing for 1 min with 1-ml aliquots of ethyl acetate, the phases were separated by centrifugation, and the organic phase was decanted and dried over anhydrous Na_2SO_4. Samples from both experiments were analyzed by GC–MS in the SIM mode for *m*/*z* 46 and *m*/*z* 47. The results of these analyses are shown in Fig. 3.

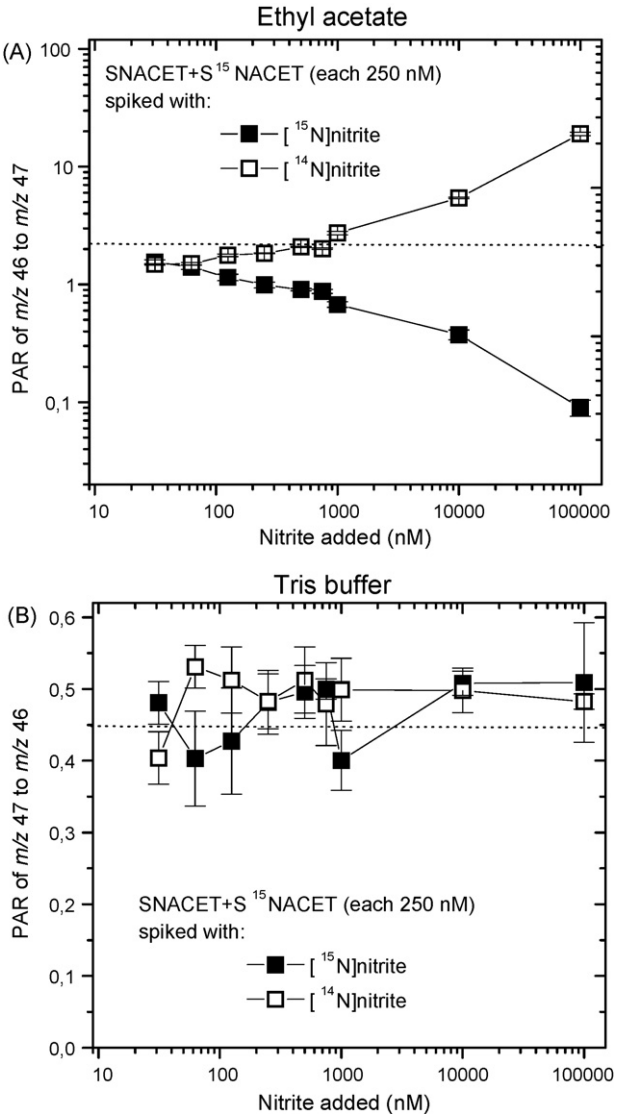

Fig. 3. Effect of addition of aqueous solutions of $[^{15}N]$nitrite and $[^{14}N]$nitrite at the indicated final added concentrations to the peak area ratio (PAR) of *m*/*z* 46 to *m*/*z* 47 (A) and of *m*/*z* 47 to *m*/*z* 46 (B) of mixtures of SNACET and S^{15}NACET (each at 250 nM) in (A) ethyl acetate and (B) in 0.2 M Tris buffer, pH 7.4. SNACET/S^{15}NACET solutions in ethyl acetate or Tris buffer were spiked with 10-μl aliquots of $[^{15}N]$nitrite and $[^{14}N]$nitrite of various concentrations. GC–MS analysis in the SIM mode was performed for *m*/*z* 47 and *m*/*z* 46. The area of the 3.3-min peak was considered in data analyses. Data are shown as mean ± SD from two independent analyses. The dotted lines indicate the PAR values in the absence of externally added $[^{15}N]$nitrite and $[^{14}N]$nitrite. Note the logarithmic scale. The HP GC–MS instrument was used.

Fig. 3A clearly shows that the presence of nitrite in ethyl acetate has a major effect of the PAR of *m*/*z* 46 to *m*/*z* 47, suggesting that under these GC–MS conditions [^{14}N]nitrite or [^{15}N]nitrite contribute considerably to compound X. Similar results were also obtained for ethyl acetate free of SNACET and S^{15}NACET. The PAR value of *m*/*z* 46 to *m*/*z* 47 in the absence of externally added nitrite was about 2.4:1, i.e., clearly distinctly different from the theoretical value of 1:1, suggesting that blank nitrite present in ethyl acetate and/or laboratory material used could have contributed to the SNACET peak to about the same extent of the order of 250 nM. On the other hand, Fig. 3B shows that nitrite externally added to Tris buffer, even at the very high concentration of 100 μM, does not contribute to compound X, because nitrite is not extracted into ethyl acetate and because the ethyl acetate used was free of water. However, the PAR value of *m*/*z* 47 to *m*/*z* 46 in the absence of externally added nitrite was about 0.44:1, i.e., clearly distinctly different from the theoretical value of 1:1, suggesting a blank nitrite of the order of 250 nM in the ethyl acetate sample. Because this order of magnitude of blank nitrite was also obtained in experiment A, it is likely that this contribution is not ascribable to aqueous nitrite but to nitrite from other contaminating sources including glass ware. Ammonium sulfamate is widely used in *S*-nitrosothiol analysis to eliminate contaminating nitrite in aqueous solution [8]. However, its use is very problematic due to the need of sample acidification and the potential artifactual formation of *S*-nitrosothiols. Because ethyl acetate but not water was found to be the source of interference, and for other method-related issues, ammonium sulfamate seems not to be useful in the present method.

We also investigated the potential contribution of organic nitrites and nitrates including butyl nitrite and glycerol trinitrate. We found that GC–MS analysis (*m*/*z* 46) of ethyl acetate solutions of these substances (0–10 μM) may considerably contribute to the compound X (data not shown).

3.1.2.3. Analysis of SNACET formed from GSNO, CysSNO or SNAC and NACET in aqueous buffered solutions. Standard curves were prepared in buffer A separately for GSNO, CysSNO and SNAC (0 nM, 200 nM, 500 nM, 750 nM and 1000 nM) using S^{15}NACET as the IS. Samples were treated in pairs for each concentration examined. The *S*-nitrosothiols were added to the 1-ml aliquots of ice-cold buffer A. After 30 s NACET (dissolved in buffer A) was added at a final concentration of 1 mM and samples were mixed by vortexing for 5 s followed by incubation for 30 s at room temperature. Subsequently, to the samples 1-ml aliquots of a 1000 nM solution of S^{15}NACET in ethyl acetate was added and the samples were mixed by vortexing for 15 s. After phase separation the ethyl acetate phase was dried over anhydrous Na_2SO_4 followed by volume reduction to about 200 μl under a stream of nitrogen. GC–MS analysis was performed by SIM of *m*/*z* 46 and *m*/*z* 47. Plotting the PAR of *m*/*z* 46 and *m*/*z* 47 (*y*) versus the *S*-nitrosothiol concentration (*x*, in μM) resulted in straight lines with the regression equations $y = 0.52 + 0.85x$ ($r = 0.9976$) for GSNO, $y = 0.67 + 0.69x$ ($r = 0.9971$) for CysSNO and $y = 0.40 + 0.51x$ ($r = 0.994$) for SNAC, suggesting considerable differences in the mean recovery rate which is estimated from the slope values to be 85% for GSNO, 69% for CysSNO and 51% for SNAC. The precision (RSD, %) of these analyses ranged between 0.4% and 10%. The reason for the different recovery rates could be that no GS^{15}NO, CysS^{15}NO or S^{15}NAC were used as respective internal standards in these analyses.

3.2. GC–MS analysis of SNACET in ethyl acetate in the presence of additives

We performed a series of experiments to test the possibility whether the method sensitivity can be enhanced by using additional compounds in the SNACET-containing ethyl acetate phase. The compounds investigated were toluene, 2-fluorobenzyl bromide, pentafluorobenzyl alcohol (PFBA) and 4-OH-TEMPO. GC–MS analysis of ethyl acetate solutions of SNACET and S^{15}NACET in the presence of these additives resulted in peaks in addition to and at the expense of compound X and compound Y, indicating that SNACET and S^{15}NACET and/or their degradation products reacted with these additives to form nitrated/nitrosated derivatives. The reaction products of SNACET/S^{15}NACET with these acceptors were identified by GC–MS as unlabelled/^{15}N-labelled α-nitro derivatives, i.e., α-nitro-toluene (t_R 5.3 min), α-nitro-2-fluorotoluene (t_R 5.1 min), α-nitro-pentafluorotoluene (t_R 4.9), and 4-hydroxy-*N*-nitroso-TEMPO (4-OH-NO-TEMPO) (t_R 4.6 min) (Fig. 4, Table 2). Presumably, the α-nitro derivatives have been formed via rearrangement of the respective nitrous acid ester. The formation of nitro and nitroso derivatives was found to be dependent upon the acceptor concentration in the ethyl acetate solution of SNACET and S^{15}NACET as shown in Fig. 5 for 4-OH-NO-TEMPO. The PAR of *m*/*z* 186 to *m*/*z* 187 (0.898 ± 0.010) did not depend upon the 4-OH-TEMPO concentration, indicating that 4-OH-NO-TEMPO and 4-OH-^{15}NO-TEMPO were formed from 4-OH-TEMPO and SNACET or S^{15}NACET at the same extent and that ^{15}N-labelled *S*-nitrosothiols may serve as internal standards. That the PAR of *m*/*z* 186 to *m*/*z* 187 deviates from the unity is most likely due to the contribution of the ^{13}C isotope of *m*/*z* 186 of 4-OH-NO-TEMPO to the *m*/*z* 187 of 4-OH-^{15}NO-TEMPO. It is worth mentioning that these derivatives had not been formed when solutions of SNACET and S^{15}NACET in solvents other than ethyl acetate such as chloroform were used (data not shown). Toluene and 2-fluorobenzyl bromide turned out to be much weaker reactants and were not considered further. PFBA and 4-OH-TEMPO allowed for a higher sensitive detection of SNACET and S^{15}NACET (data not shown) and were used both at a final concentration of 1 mM in ethyl acetate solutions in quantitative analyses. As the 4-OH-NO-TEMPO derivative was detectable only in the EI mode, we converted 4-OH-NO-TEMPO to its pentafluorobenzoic acid ester derivative using pentafluorobenzoyl chloride as the acylation reagent (Table 2). This in-injector derivatization allows for a more sensitive detection of SNACET in the NICI mode as compared to the EI mode (data not shown).

Separate standard curves for GSNO (0 nM, 62.5 nM, 125 nM, 250 nM, 500 nM, 750 nM and 1000 nM; in triplicate for each concentration) and ALB-SNO (0 nM, 50 nM, 100 nM, 200 nM, 300 nM, 400 nM and 600 nM; in duplicate for each concentration) were prepared in buffer B using GS^{15}NO and ALB-S^{15}NO as the internal standards at fixed concentrations of 250 nM and 280 nM, respectively. After conversion of NACET (at 0.1 mM) to SNACET and extraction with ethyl acetate, PFBA (in ethyl acetate) was added (at 1 mM) and samples were analyzed by GC–MS. In case of ALB-SNO samples were also analyzed by a previously described method based on the use of $HgCl_2$ [14]. Linear relationships were observed by plotting the PAR of *m*/*z* 46 to *m*/*z* 47 (*y*) versus the concentration of GSNO or ALB-SNO (*x*). The regression equation from GSNO analysis was $y = 0.238 + 0.0047x$ ($r = 0.9995$). The regression equations from ALB-SNO analyses were $y = 0.064 + 0.0032x$ ($r = 0.9959$) using NACET and PFBA (i.e., the present method), and $y = 0.062 + 0.0030x$ ($r = 0.9992$) using $HgCl_2$ (i.e., the previous method [14]). In pairs comparison of the PAR of *m*/*z* 46 to *m*/*z* 47 obtained by both methods resulted in the ratio of 1.045 ± 0.135. These observations indicate that both methods are fairly comparable each other with regard to ALB-CysSNO. The precision (RSD, %) of the method using NACET and PFBA ranged between 17% for unspiked samples and 0.9% for the highest spikes for GSNO and ALB-CysSNO.

3.3. S-Nitrosothiol analysis in human plasma in vitro

The procedures described above for buffered solutions of *S*-nitrosothiols were found to be applicable to human plasma from

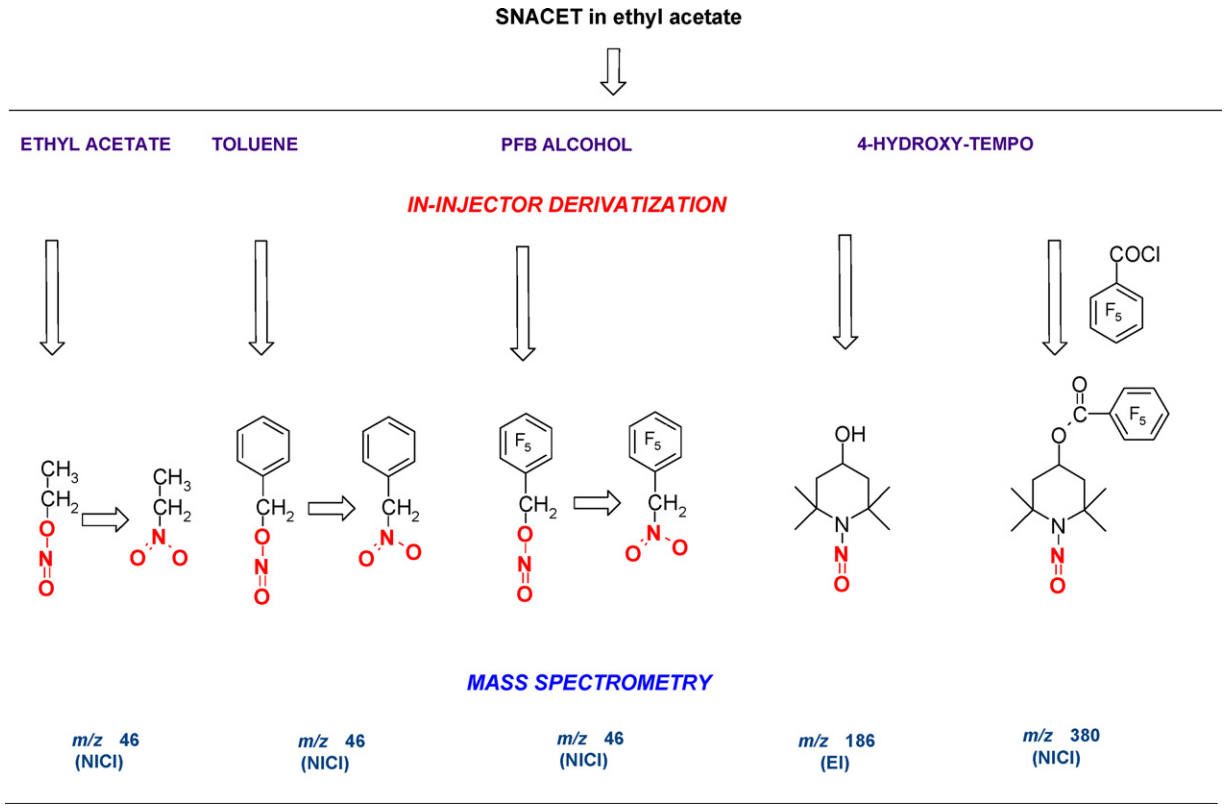

Fig. 4. Proposed structures for derivatives formed during "in-injector derivatization" at an injector temperature of 250 °C of SNACET in ethyl acetate in the absence or in the presence of the acceptors toluene, pentafluorobenzyl (PFB) alcohol and 4-hydroxy-TEMPO. GC–MS analyses were performed in the negative-ion chemical ionization (NICI) and electron ionization (EI) mode. It is assumed that the initially formed nitrous acid esters rearrange to form the respective nitro derivatives. The *m/z* values shown at the bottom are suitable for quantitative analyses.

EDTA-anticoagulated blood. However, several experimental conditions required appropriate modification in order to take into account specific conditions prevailing in plasma as compared to buffered aqueous solutions, despite the use of ^{15}N-labelled *S*-nitrosothiols as internal standards. Parameters to be considered and optimized for plasma analyses were (1) NACET concentration to be added; (2) stabilization of *S*-nitrosothiols in plasma samples in which they are considerable less stable as compared to

Table 2
Major ions (intensity ≥ 10%) present in the GC–MS mass spectra of non-derivatized and derivatized 4-OH-TEMPO and 4-OH-NO-TEMPO produced from 4-OH-TEMPO and SNACET or S^{15}NACET[a].

Non-derivatized			
4-OH-TEMPO *m/z* (intensity, %) electron ionisation	4-OH-NO-TEMPO	4-OH-^{15}NO-TEMPO	Ion assignment
41 (90)	41 (50)	41 (48)	$[C_3H_5]^+$
57 (75)	57 (100)	57 (100)	$[C_3H_5O]^+$
71 (100)	71 (30)	71 (30)	$[(CH_3)_2C–CH_2–CH_3]^+$
85 (25)	85 (75)	85 (75)	$[(CH_3)_2C–CH(CH_3)_2]^+$
N.D.	156 (10)	156 (10)	$[M–NO/M–^{15}NO]^+$
172 (15)	N.D.	N.D.	$[M]^+$
N.D.	186 (33)	187 (30)	$[M]^+$

Pentafluorobenzoic acid esters		
4-OH-TEMPO electron ionization *m/z* (intensity, %)/ion	4-OH-TEMPO	4-OH-NO-TEMPO/4-OH-^{15}NO-TEMPO
	Electron capture negative-ion chemical ionization	
109 (61)/N.I.	N.D.	N.D.
124 (57)/N.I.	N.D.	N.D.
140 (42)/N.I.	N.D.	N.D.
167 (20)/$[C_6F_5]^+$	N.D.	N.D.
N.D.	178 (12)/N.I.	N.D.
195 (100)/$[C_6F_5CO]^+$	196 (23)/N.I.	N.D.
N.D.	N.D.	335 (10)/336 (12)/$[M–HCOOH]^+$
352 (18)/$[M–16]^+$	351 (13)/$[M–17]^+$	N.D.
368 (20)/$[M]^+$	367 (100)/$[M–H]^+$	N.D.
N.D.	N.D.	380 (100)/381 (100)/$[M–H]^+$

N.D., not detected; N.I., not identified.
[a] The relative retention time of 4-OH-TEMPO and 4-OH-NO-TEMPO was 0.85 and 1.02 with respect to NACET. The HP instrument was used; the injector temperature was 250 °C.

buffer, notably in the nM-range; (3) inhibition of esterase activity for maximum yield of SNACET; (4) incubation and vortex time to allow maximum *S*-transnitrosation combined with minimum loss of SNACET and other *S*-nitrosothiols; (5) volume of plasma and ethyl acetate to ensure quantitative analyses in a relevant concentration range—assumed to be below 1 μM [8,9]; and (6) the potential need for an acceptor in the ethyl acetate extract. Eventually, in consideration of the heterogeneity of *S*-nitrosothiols in human plasma, of the goal of the study aiming to measure the sum of *S*-nitrosothiols via *S*-transnitrosation to SNACET by NACET, and of the by far easier synthesis, structural characterization and quantitative standardization of LMM *S*-nitrosothiols, we used GSNO/GS^{15}NO and SNACET/S^{15}NACET as model *S*-nitrosothiols. Independently of other experimental parameters, the minimum volume of ethyl acetate used for extraction of SNACET/S^{15}NACET formed in plasma was twice that of the plasma volume for the purpose of easier phase separation. Also, a final NACET concentration in plasma samples of 1 mM was found to be necessary and satisfactory to ensure maximum recovery of SNACET/S^{15}NACET by keeping NACET in molar excess over disulfides and other reducible functionalities in the plasma.

For added final plasma concentrations up to 10 μM for GSNO/GS^{15}NO and SNACET/S^{15}NACET, no use of chelators such as DTPA, esterase inhibitors such as PMSF or additives such as PFBA was required. Indeed, linear relationships were observed between the PAR of *m*/*z* 46 to *m*/*z* 47 (*y*) measured (compound X) and the concentration (*x*) of GSNO or SNACET added to plasma (1 ml; final concentrations 0 μM, 0.5 μM, 1 μM, 2.5 μM, 5 μM, 7.5 μM and 10 μM) using GS^{15}NO (25 μM) or S^{15}NACET (10 μM) as internal standards: $y = 0.17 + 0.043x$ ($r = 0.9912$) for GSNO and $y = 0.22 + 0.096x$ ($r = 0.9983$) for SNACET. The RSD values in these analyses ranged between 13% for unspiked and 0.2% for spiked plasma samples. The *y*-axis intercepts suggest presence of *S*-nitrosothiols in the unspiked plasma used at basal concentrations of about 4.3 μM and 2.2 μM, respectively, but this order of magnitude was also observed in buffer B, as already mentioned above, and is most likely due to blank (see below). The values of the slope differ because of the use of different concentrations for the internal standard.

Under these conditions (i.e., no NACET, no acceptor) we tested the applicability of the method to human plasma spiked with d_3-S^{15}NACET (0–10 μM), with SNACET serving as the IS at 10 μM. Linear regression analysis between measured and added d_3-S^{15}NACET resulted in the regression equations: $y_1 = 0.27 + 1.05x_1$ ($r_1 = 0.9981$) for compound X (i.e., from measuring PAR of *m*/*z* 47 to *m*/*z* 46) and $y_2 = 1.09 + 1.21x_2$ ($r_2 = 0.9943$) for compound Y (i.e., from measuring PAR of *m*/*z* 160 to *m*/*z* 157). Thus, the straight lines observed are fairly parallel for compound X and compound Y. These results indicate almost quantitative recovery of d_3-S^{15}NACET from plasma.

3.3.1. *Effect of esterase activity on S-nitrosothiol analysis*

Being esters, it may be expected that NACET and SNACET will be readily hydrolyzed by esterases which are abundantly present in human plasma. Thus, esterase activity in plasma could be the source for considerable loss of SNACET formed from endogenous *S*-nitrosothiols and NACET by *S*-transnitrosation. Indeed, using a commercially available esterase we showed that in buffer A esterase activity may considerably decrease the SNACET concentration at room temperature, with the rate and extent of the decrease being dependent upon esterase activity, incubation time, and initial SNACET concentration (data not shown). In the presence of PMSF, a non-specific esterase inhibitor, SNACET decrease was inhibited in a concentration-dependent manner as measured by SIM of *m*/*z* 46, *m*/*z* 47, *m*/*z* 157 and *m*/*z* 160. In SNACET solutions in buffer A, a PMSF concentration of 100 μM was sufficient to completely inhibit esterase-catalyzed (activity, up to 72 mU/ml) hydrolysis of SNACET for up to 30 min of incubation at room temperature. By contrast, in plasma PMSF was much less potent as an esterase inhibitor so that PMSF concentrations higher than 1 mM were necessary to enhance SNACET stability in this esterases-rich matrix. Interestingly, we found that DTPA alone was also able to abolish SNACET decrease in human plasma in a concentration-dependent manner (Fig. 6). Therefore, quantitative analysis of *S*-nitrosothiols in plasma was commonly performed by adding only DTPA to plasma at a final concentration of 1 mM. The mechanism by which DPTA inhibits esterase activity in human plasma remains to be investigated.

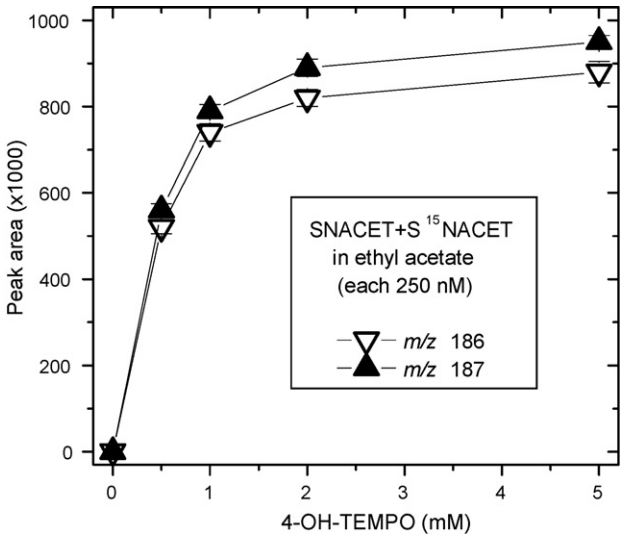

Fig. 5. Effect of the 4-OH-TEMPO concentration on the formation of unlabelled (*m*/*z* 186) and ^{15}N-labelled (*m*/*z* 187) *N*-nitroso-4-OH-TEMPO from SNACET (250 nM) and S^{15}NACET (250 nM) in ethyl acetate. GC–MS analyses were performed in the electron ionization (EI) mode on the HP instrument, see Table 2 and Fig. 4.

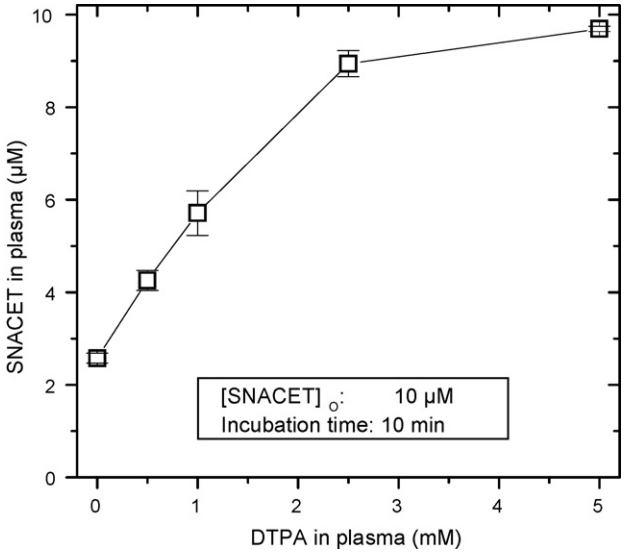

Fig. 6. Effect of DTPA on the stability of SNACET in human plasma. To human plasma samples DTPA was added to reach final added concentrations of 0 mM, 0.5 mM, 1 mM, 2.5 mM and 5 mM. The experiment was started by the addition of SNACET at a final concentration of 10 μM each. After 10 min of incubation at room temperature, 2-ml aliquots of a d_3-S^{15}NACET (10 μM) solution in ethyl acetate were added to all samples. The samples were mixed by vortexing for 30 s and analyzed by GC–MS in the SIM mode (*m*/*z* 46 and *m*/*z* 47) after phase separation and drying the ethyl acetate phase over anhydrous Na_2SO_4. Data are shown as mean ± SD from two independent measurements. The HP instrument was used.

3.3.2. Accuracy and precision of the method for SNACET and GSNO in the range of 0–10 μM in human plasma

The analytical performance of the method for SNACET (at added final concentrations of 0 μM, 2 μM, 4 μM, 6 μM, 8 μM and 10 μM) in a pooled human plasma (each 100 μl aliquots in quadruplicate) was examined without the use of any additional reagents or chemicals in the plasma or ethyl acetate (200 μl) except for the internal standard d_3-S^{15}NACET which was used in ethyl acetate at a final concentration of 10 μM. In order to avoid loss of SNACET and d_3-S^{15}NACET, samples were analyzed in pairs for each concentration examined until the phase separation step. Upon addition to the plasma samples and brief vortex-mixing, samples were extracted with ethyl acetate by vortex-mixing for 30 s, the phases were separated by centrifugation and the decanted ethyl acetate phase was dried over anhydrous Na_2SO_4. GC–MS analysis was performed by SIM of *m*/*z* 46, *m*/*z* 47, *m*/*z* 157 and *m*/*z* 160 of all samples from an experiment ($n = 24$) within a run after generation of the last four samples of each experiment. The first series was performed using distilled water (on day −4), the other three series on pooled plasma which had been portioned to 100-μl aliquots before (on days 1, 4 and 5), i.e., within a period of 10 days in total. Also, all SNACET and d_3-S^{15}NACET solutions used for spiking had been freshly prepared; SNACET and d_3-S^{15}NACET solutions were discarded after use. The results of these experiments are shown in Fig. 7 and their statistical evaluation is summarized in Table 3. Typical chromatograms from GC–MS analyses of SNACET in human plasma without and with external addition of 10 μM SNACET are shown in Fig. 8. It is worth mentioning that high imprecision was noted for the unspiked samples presumably due to varying interference by nitrite and in part to the fact that d_3-S^{15}NACET was used in ethyl acetate.

GSNO (to reach final added concentrations of 0 μM, 2 μM, 5 μM, 7.5 μM and 10 μM) was used as an additional model *S*-nitrosothiol for quantitative analyses in human plasma. For this, human pooled plasma was spiked with DTPA (10 μl, 100 mM) at a final added concentration of 1 mM. After addition of GSNO (0–10 μl, 1 mM) to two 1-ml plasma aliquots for each concentration point, NACET (10 μl, 100 mM) was added and samples were incubated for 1 min after brief vortex-mixing. Samples were then extracted by vortex-mixing for 30 s with 2 ml of ethyl acetate that contained 10 μM of d_3-S^{15}NACET. After phase separation by centrifugation and drying

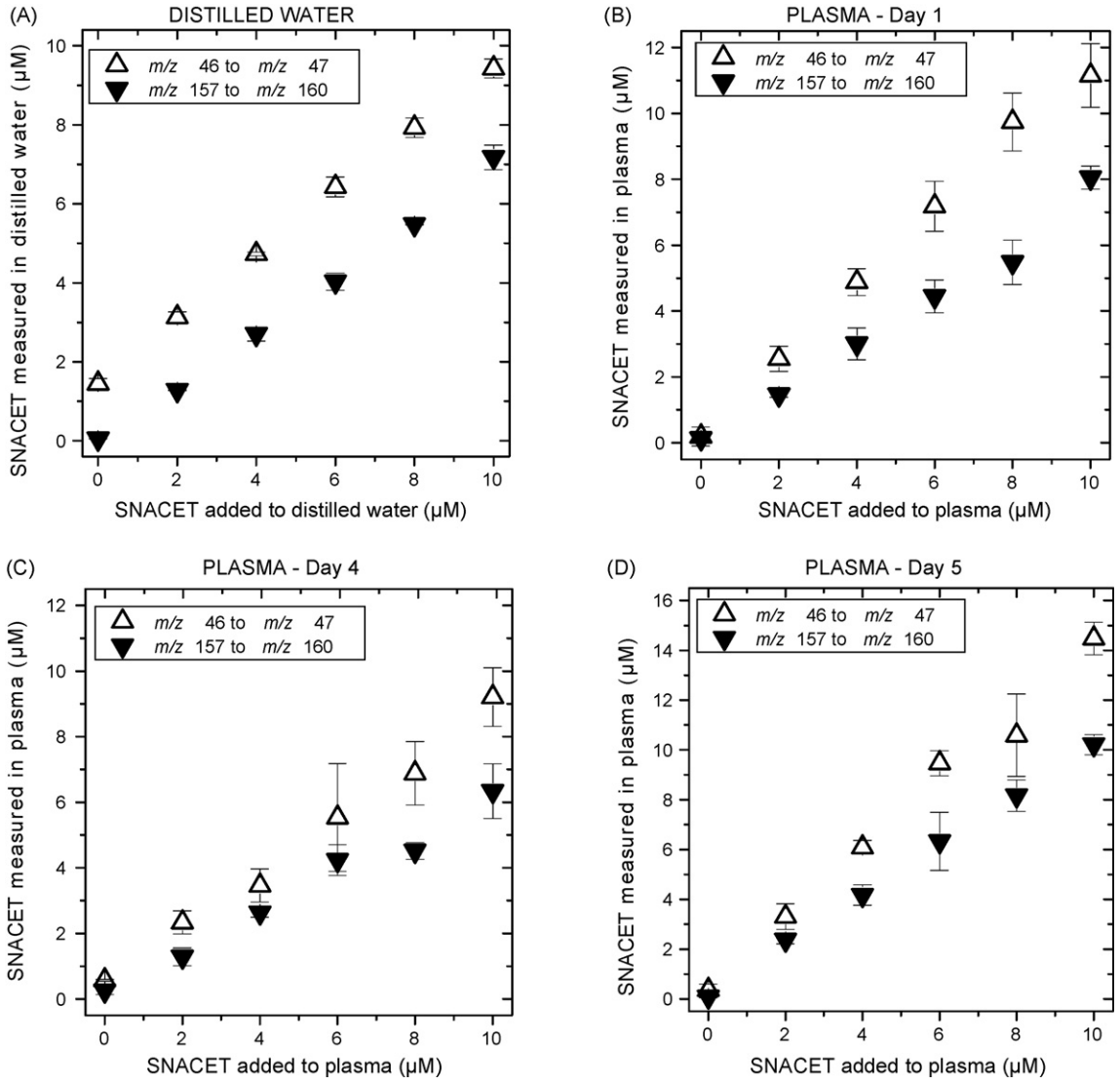

Fig. 7. Relationship between SNACET measured and SNACET added (0–10 μM) to distilled water (A, 100 μl aliquots) and human plasma (B–D, 100 μl aliquots) on 4 days within an interval of 10 days using d_3-S^{15}NACET as the internal standard (10 μM). All analyses were performed in quadruplicate and in pairs for each concentration examined. Samples were extracted with 200-μl aliquots of ethyl acetate. GC–MS analyses were performed by SIM of *m*/*z* 46, *m*/*z* 47 (compound X), *m*/*z* 157 and *m*/*z* 160 (compound Y) on the DSQ instrument. No additives were used in this series. SNACET concentration was calculated by multiplying the respective peak area ratio by the SNACET d_3-S^{15}NACET concentration. The statistical evaluation is summarized in Table 3.

Table 3
Statistical evaluation of the GC–MS standard curves of SNACET (0–10 μM) prepared in distilled water and in human plasma using d_3-S^{15}NACET (10 μM) as internal standard.

Day[a]	From *m*/*z* 46 to *m*/*z* 47 (compound X)[b]			From *m*/*z* 157 to *m*/*z* 160 (compound Y)[c]			Matrix
	$y = a + bx$[d]	*r*	RSD (%)[e]	$y = a + bx$[d]	*r*	RSD (%)[e]	
−4	$y = 1.52 + 0.80x$	$r = 0.999$	1–9	$y = -0.09 + 0.71x$	$r = 0.999$	2–25	Distilled water
1	$y = 0.33 + 1.12x$	$r = 0.998$	9–145	$y = -0.03 + 0.76x$	$r = 0.993$	4–58	Human plasma
4	$y = 0.54 + 1.37x$	$r = 0.995$	5–62	$y = 0.21 + 1.00x$	$r = 0.999$	4–53	Human plasma
5	$y = 0.46 + 0.84x$	$r = 0.996$	5–30	$y = 0.23 + 0.60x$	$r = 0.991$	6–47	Human plasma

[a] Analyses were performed within an interval of 10 days. Samples were analyzed in pairs in quadruplicate for each concentration point.
[b] SIM of *m*/*z* 46 to *m*/*z* 47 for compound X performed on the DSQ instrument.
[c] SIM of *m*/*z* 157 to *m*/*z* 160 for compound Y performed on the DSQ instrument.
[d] Regression equations were generated from linear regression analysis between measured (*y*) and added (*x*) SNACET.
[e] Minimum and maximum RSD values observed in the whole concentration range.

the ethyl acetate phase over anhydrous Na_2SO_4, solvent volume was reduced to about 300 μl by means of a nitrogen stream. All samples were treated in pairs until the centrifugation step. Linear regression analysis between the PAR of *m*/*z* 46 to *m*/*z* 47 (*y*) measured and the GSNO concentration (*x*) added to plasma (in μM) led to the regression equation $y = 0.134 + 0.111x$ ($r = 0.9998$). The precision (RSD) with which these analyses were performed ranged between 0% and 8%. The reciprocal of the slope value of the regression equation provides a mean value of 9 μM for the internal standard d_3-S^{15}NACET, which deviates by about −10% from the nominal value of 10 μM. From the *y*-axis intercept value of 0.134 an apparent basal total concentration of plasma RSNO of 1.34 μM is calculated (see next section).

3.3.3. *Quantification of exogenous GSNO in the range of 0–1000 nM in human plasma*

Using the experimental procedures described above, including use of 1-ml plasma volume, 1 mM DTPA and 1 mM NACET, incuba-

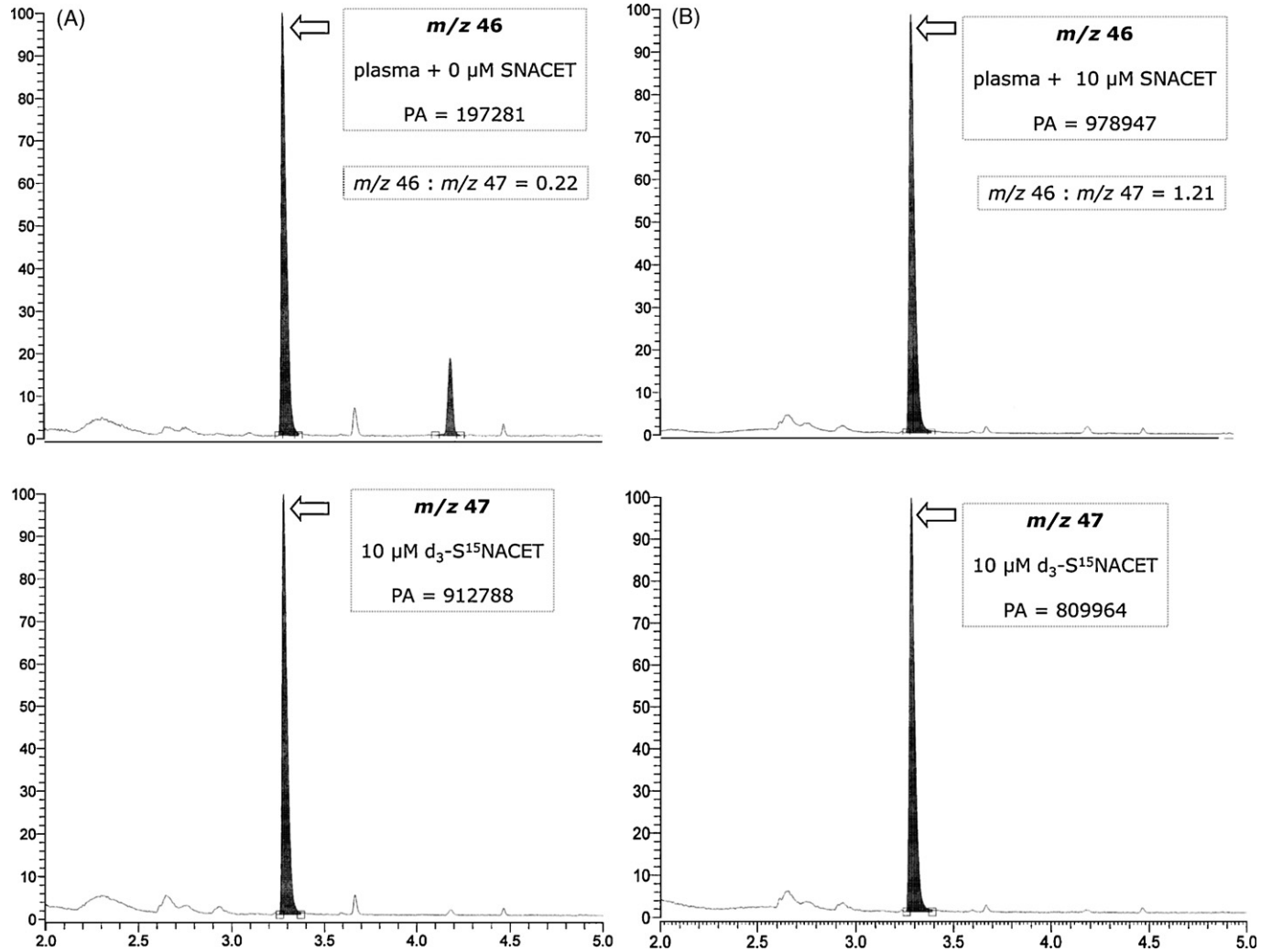

Fig. 8. GC–MS chromatograms from the analysis of total *S*-nitrosothiols in plasma before (A) and after (B) addition of SNACET at a final added concentration of 10 μM. d_3-S^{15}NACET was used as the internal standard at 10 μM with respect to plasma (1 ml). The internal standard was supplied in ethyl acetate (2 ml). GC–MS analyses were performed in the NICI mode by SIM of *m*/*z* 46 and *m*/*z* 47 (compound X) on the DSQ instrument. *y*- and *x*-axes show relative intensity (%) and retention time (min). The solid peak at about 4.18 min was not investigated.

Table 4
Analytical performance of the GC–MS[a] method for GSNO added to human plasma in the range of 0–1000 nM using d_3-SNACET as internal standard at 1000 nM.

GSNO added (nM)	Peak area ratio of *m/z* 46 to *m/z* 47, mean ± SD (RSD, %; *n* = 2)			
	Day 1a (January 9)	Day 1b (January 9)	Day 2 (January 11)	Day 3 (March 10)
0	0.412 ± 0.033 (8.0)	0.452 ± 0.003 (0.7)	0.495 ± 0.061 (12.3)	0.590 ± 0.024 (4.1)
200	0.528 ± 0.041 (7.8)	0.599 ± 0.037 (6.2)	0.634 ± 0.034 (5.4)	0.658 ± 0.086 (13.1)
500	0.613 ± 0.026 (4.2)	0.684 ± 0.016 (2.3)	0.736 ± 0.036 (4.9)	0.758 ± 0.029 (3.8)
750	0.736 ± 0.051 (6.9)	0.800 ± 0.049 (6.1)	0.862 ± 0.005 (0.6)	0.875 ± 0.036 (4.1)
1000	0.960 ± 0.001 (0.1)	0.966 ± 0.105 (10.9)	0.980 ± 0.050 (5.1)	0.994 ± 0.025 (2.5)
Regression eq.	*y* = 0.400 + 5.1E−4*x*	*y* = 0.465 + 4.8E−4*x*	*y* = 0.512 + 4.7E−4*x*	*y* = 0.578 + 4.0E−4*x*
Correlation coeff.	*r* = 0.9793	*r* = 0.9897	*r* = 0.9958	*r* = 0.9962

[a] The DSQ instrument was used.

tion time of 60 s and extraction time of 30 s, we applied the method to quantify GSNO spiked to human plasma to reach final added concentrations of 0 nM, 200 nM, 500 nM, 750 nM and 1000 nM using d_3-S^{15}NACET (1000 nM in ethyl acetate) as internal standard. Analyses were performed on 3 days; all samples were treated in pairs until the centrifugation step. Except for the pooled plasma, which was stored frozen at −80 °C in 1-ml portions, all other solutions were prepared freshly. The regression equations and correlation coefficients obtained from linear regression analysis of the PAR of *m/z* 46 to *m/z* 47 (*y*) versus the GSNO concentration (*x*) added to plasma (in nM) are summarized in Table 4. The correlation coefficients were fairly comparable and equal or higher than 0.98, indicating satisfactory linearity in this concentration range. Also, the precision (RSD) of the method was analytically acceptable for each GSNO concentration examined (range, 0.1–13.1%). By contrast, the *y*-axis intercept varied considerably suggesting that the sum of the *S*-nitrosothiols present in the plasma is about 400–600 nM. Interestingly, these values are 2–3 times smaller than the value of 1340 nM obtained in the range 0–10 μM of GSNO (see preceding section), although the same pooled plasma was used in the measurements. The reciprocal of the slope values of the regression equations of Table 4 provides mean values of 1960 nM, 2080 nM, 2130 nM and 2500 nM for the internal standard d_3-S^{15}NACET. These values deviate by about 200–250% from the nominal value of 1000 nM. Plotting the mean PAR (*y*) of the data of Table 4 versus the GSNO concentration (*x*) added resulted in the regression equation *y* = 0.485 + 0.00049*x* (*r* = 0.9963) which provides 485 nM for basal *S*-nitrosothiols in total and 2040 nM for the internal standard d_3-S^{15}NACET. Taken together, these results indicate severe analytical problems with the measurement of *S*-nitrosothiols in human plasma by this method in parts due to contaminating nitrite.

3.4. Pharmacokinetics and metabolism of orally administered S^{15}NACET in the rabbit

By means of the present method orally administered S^{15}NACET (62.6 nmol/kg bw) could not be detected in rabbit plasma in any of the plasma samples taken over the whole observation period (4–240 min), although blood samples were extracted immediately. In the present study we used a previous GC–MS method for measuring ALB-S^{15}NO which is based on the use of $HgCl_2$ [14], because we expected formation of ALB-S^{15}NO at very low concentrations and because the previously reported GC–MS method is less affected by interfering nitrite than the present method. In other respects the present and the previous GC–MS method [14] provided comparable results for ALB-SNO. Thus, plotting of the PAR of *m/z* 46 to *m/z* 47 measured for ALB-SNO (0 pmol, 50 pmol, 100 pmol, 200 pmol, 300 pmol, 400 pmol and 600 pmol; each 280 pmol of ALB-S^{15}NO as IS) using the present method (*y*) versus the PAR of *m/z* 46 to *m/z* 47 measured by the method using $HgCl_2$ [14] (*x*) resulted in the regression equation *y* = −0.001 + 1.07*x*, *r* = 0.9947. In contrast to S^{15}NACET we detected ALB-S^{15}NO in rabbit plasma at a maximum concentration of about 90 nM after 20 min of administration (Fig. 9A). Presumably, the plasma concentration of ALB-S^{15}NO was higher at earlier time points. The highest plasma concentrations were measured for [^{15}N]nitrate and [^{15}N]nitrite, with the pharmacokinetics of which being apparently clearly different each other (Fig. 9B). Thus, the concentration time curve of [^{15}N]nitrite shows a maximum concentration of about 10 μM 20 min after administration, whereas the [^{15}N]nitrate concentration was relatively constant

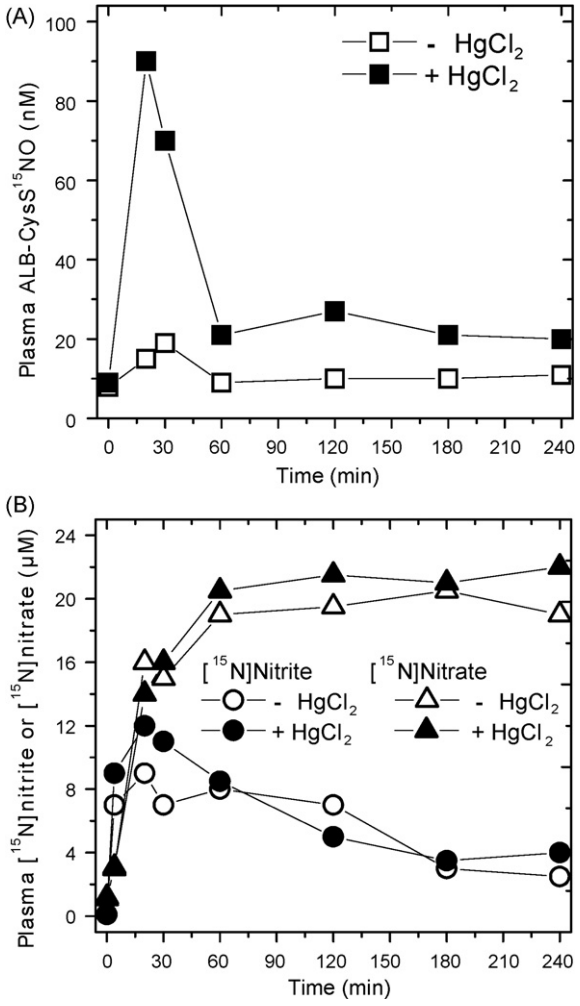

Fig. 9. Concentration time course of (A) ALB-S^{15}NO and (B) [^{15}N]nitrite and [^{15}N]nitrate in plasma samples of a rabbit before and after oral administration of 62.6 nmol S^{15}NACET per kg body weight. Note that due to the natural occurrence of the ^{15}N isotope (0.36%) the concentration of ALB-S^{15}NO, [^{15}N]nitrite and [^{15}N]nitrate in the plasma sample before S^{15}NACET administration is not zero. GC–MS analyses were performed in the NICI mode by SIM of *m/z* 46 and *m/z* 47 on the HP instrument as described [22].

at about 20 μM after 60 min of administration. Plasma concentrations of [^{15}N]nitrite and [^{15}N]nitrate were calculated by using the basal plasma concentrations of nitrite (i.e., 22.2 ± 0.4 μM, n = 2) and nitrate (i.e., 137 ± 1.7 μM, n = 2), which were considered constant in all plasma samples analyzed. Plasma concentrations of [^{15}N]nitrite and [^{15}N]nitrate 60 min after oral administration of S^{15}NACET in another two rabbits were 1.1 μM and 1.4 μM for [^{15}N]nitrite and 5.3 μM and 6.4 μM for [^{15}N]nitrate, at doses of 40.3 nmol/kg bw and 44.6 nmol/kg bw, respectively, i.e., considerably lower as compared to the higher dose of 62.6 nmol/kg bw.

4. Discussion

4.1. Mechanistic aspects

From the analytical point of view, endogenous HMM and LMM *S*-nitrosothiols are very challenging in many biological fluids and tissues, notably in blood. Both concentrations and functions of *S*-nitrosothiols have been and are still subject of controversial discussion in the literature [6,8,9,23–33]. Many of the identified and recognized analytical problems and pitfalls clearly arise from the chemical nature of *S*-nitrosothiols. These particular problems are difficult to control. Other problems associated with the analysis of these compounds seem to be related to the scientists themselves, i.e., to their rather hesitant preparedness to develop reliable, i.e., interference- and pitfall-free analytical methods, to validate them adequately and to test their appropriateness carefully prior to use in quantitative analyses in basic and clinical research [8,9,29,33]. This kind of problem is considered *homemade* and should be therefore avoidable.

To the best of our knowledge, until the present day there is only one reported method that allows for direct quantitative determination of a single *S*-nitrosothiol, i.e., GSNO, in human plasma. This method is based on LC–MS/MS analysis of GSNO in the supernatant of acetonitrile-treated plasma and provides basal plasma levels of about 300 pM [13]. This concentration is presumably the lowest reported value for an endogenous *S*-nitrosothiol in human plasma in the basal state thus far [32]. Unfortunately, this LC–MS/MS method has not been reported in detail [13] and its analytical performance cannot be adequately evaluated [32]. With this sole exception, all other reported methods for *S*-nitrosothiols are indirect and require conversion of the *S*-nitroso group into analytes such as nitrite, nitrate or NO for subsequent detection [8,9]. Because of the ubiquity of nitrite, nitrate and NO – the latter and its higher oxides (NO_x) being present in exhaled air and in the atmosphere as pollutants – at concentrations comparable to or even higher than those of endogenous *S*-nitrosothiols, accurate quantitative determination of *S*-nitrosothiols in plasma, serum, erythrocytes and whole blood is an extraordinarily difficult endeavor. Presumably, analytical difficulties rather than other reasons such as photoinstability have led to an almost 5 order of magnitude wide concentration range for endogenous *S*-nitrosothiols in human plasma [33].

Driven by the initial report on the occurrence of ALB-SNO at basal concentrations of about 7 μM in plasma of healthy humans [3], we developed GC–MS methods for this particular HMM *S*-nitrosothiol in combination with its specific affinity column extraction from plasma, conversion into nitrite either by $HgCl_2$ [14] or Cu^{2+}/cysteine [15], followed by derivatization to the pentafluorobenzyl derivative and quantification by GC–MS using ALB-S^{15}NO as the internal standard. These methods revealed basal ALB-SNO plasma concentrations of about 160 nM in humans [14,15]. Because this value is 2 times smaller than the concentration of nitrite present as contamination in buffer B of the affinity extraction, and because the limit of quantitation (LOQ) value of the method is quite high, i.e., about 100 nM [14], these GC–MS methods do not allow detection of small changes in ALB-SNO plasma concentrations. Nevertheless, we think that these GC–MS methods provide convincing evidence that the ALB-SNO concentration in plasma of healthy humans and those suffering from renal and hepatic diseases is not higher than about 200 nM [14].

In consideration of the extant disagreement concerning basal plasma levels of *S*-nitrosothiols in humans and mammals we were interested in developing alternative methods for the quantitative determination of *S*-nitrosothiols in human plasma in total. The most useful method appeared to be the conversion of all plasma *S*-nitrosothiols into a single *S*-nitrosothiol via the specific *S*-transnitrosation reaction according to Eq. (2). For this we synthesized and used the novel exogenous LMM thiol NACET, i.e., *N*-acety-L-cysteine ethyl ester. In contrast to endogenous thiols, NACET, as well as the corresponding *S*-nitroso derivative, i.e., SNACET (i.e., a red colored oily substance), is highly miscible both with water and with most water-immiscible organic solvents including ethyl acetate and chloroform. Theoretically, use of organic solvents would allow the separation of SNACET from the major contaminating and interfering species, i.e., nitrite, and therefore the elimination of problems arising from this ubiquitous anion. Indeed, we found that both NACET and SNACET are quantitatively extracted from aqueous buffered solutions into organic solvents such as ethyl acetate and chloroform (data not shown). As MS-based techniques are unique in using stable-isotope labelled analogs of analytes, and in order to be able to compare the novel method with existing methods previously reported by us [14,15], we decided to use the GC–MS technique in combination with the use, as internal standards, of stable-isotope labelled analogs of SNACET, i.e., the simply labelled S^{15}NACET and the doubly labelled d_3-S^{15}NACET, with the ^{15}N-label being in the *S*-nitroso group and the deuterium-label in the *N*-acetyl group, respectively.

Being an electrically neutral molecule, SNACET does not require any derivatization for analysis by GC–MS, unlike its free acid, i.e., SNAC [19]. On the other hand and despite considerable volatility of SNACET, given the thermal lability of the *S*-nitroso group, intact SNACET could not be detected by GC–MS. When SNACET, S^{15}NACET and d_3-S^{15}NACET were analyzed by injecting into the GC–MS apparatus their ethyl acetate solutions, we observed two major peaks in dependence on the injector temperature between 200 °C and 300 °C (Fig. 2). These peaks were absent when other solvents such as chloroform were used. We could not definitely elucidate the structure of the species produced by thermal degradation within the injector in the presence of ethyl acetate. Two GC peaks were of considerable analytical interest, i.e., the compound X (t_R, 3.3 min) and compound Y (t_R, 5.2 min), because under NICI conditions they ionize to m/z 46 and m/z 47 (from compound X), and to m/z 157 (from SNACET and S^{15}NACET) and to m/z 160 (from d_3-S^{15}NACET), respectively, suggesting that these species could be utilized for quantitative analyses. In the presence of additional compounds with the potential of nitration and nitrosation, e.g., toluene, pentafluorobenzyl alcohol and 4-HO-TEMPO (Fig. 5), injection of SNACET solutions in ethyl acetate resulted in elution of additional peaks of nitro and nitroso groups-containing derivatives. Again, these peaks were absent when other solvents such as chloroform were used. These findings strongly suggest that ethyl acetate catalyzes the formation of α-nitro-toluene, α-nitro-pentafluoro-toluene and *N*-nitroso-4-OH-TEMPO (i.e., 4-OH-NO-TEMPO). It is possible that initially the nitrous acid esters are formed which then rearrange to form the nitro derivatives as has been observed for the nucleophilic substitution of bromide in pentafluorobenzyl bromide by nitrite [22]. Presumably, in the absence of any acceptor in ethyl acetate, SNACET forms the nitrous ester of ethanol, i.e., CH_3CH_2O–N=O, which rearranges to $CH_3CH_2NO_2$ that mainly ionizes to form nitrite. Thus, compound X could be $CH_3CH_2NO_2$ (Fig. 4). It is worth mentioning that GC–MS analysis of compound X requires a low oven tem-

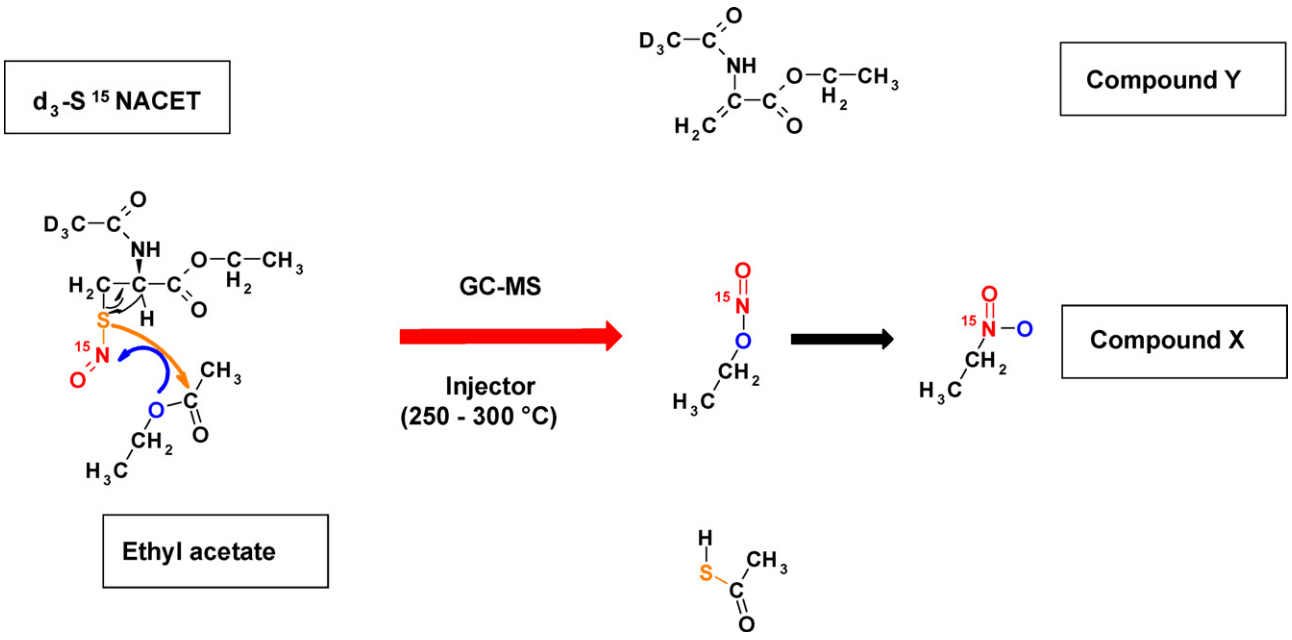

Fig. 10. Proposed mechanism for the formation of compound X and compound Y from d_3-S^{15}NACET and ethyl acetate within the injector of the GC–MS instruments used at injector temperatures of 250–300 °C. For more details see the text.

perature of 40 °C at the start, which supports the volatility and the identity of compound X as $CH_3CH_2NO_2$. It is noteworthy that $CH_3CH_2NO_2$ has a boiling point of about 114 °C, which is very close to that of toluene (111 °C). Because compound Y emerges from the GC column later than compound X and close to NACET, and its mass spectrum does not contain ions due to nitrite (i.e., *m*/*z* 46), it is likely that compound Y results from decomposition of the *S*-nitroso group of SNACET (Fig. 4). That ethyl acetate is required for the formation of nitrated and nitrosated derivatives from SNACET is supported by the finding that trifluoroacetic anhydride catalyzes the nitration of toluene [34]. A mechanism for the formation of compound X and compound Y is proposed in Fig. 10 for d_3-S^{15}NACET.

4.2. Applications of the method—quantitative aspects

Quantitative analyses were performed by SIM of *m*/*z* 46 and *m*/*z* 47 (for compound X) and of *m*/*z* 157 and *m*/*z* 160 (for compound Y) for unlabelled and labelled *S*-nitrosothiols. The applicability of the method was shown for SNACET itself and for SNACET formed in aqueous buffered solutions or plasma from various LMM *S*-nitrosothiols and ALB-SNO in vitro and in vivo via *S*-transnitrosation of NACET (Eq. (3)).

In vivo, upon oral administration of S^{15}NACET to rabbits, no intact S^{15}NACET (directly extracted from blood with ethyl acetate) could be detected in any of the blood samples taken. By contrast, we detected formation of ALB-S^{15}NO at a concentration of about 90 nM after 20 min of administration and rapid formation of [^{15}N]nitrite and [^{15}N]nitrate in the low μM-range (Fig. 9). These findings suggest that SNACET may serve as an NO-releasing and NO^+ groups-transferring pro-drug. Interestingly, the kinetics of [^{15}N]nitrite and [^{15}N]nitrate differ clearly each other, whereas changes in plasma concentrations of [^{15}N]nitrite and ALB-S^{15}NO seem to occur synchronously. [^{15}N]Nitrite and [^{15}N]nitrate were formed at similar concentrations–the [^{15}N]nitrite:[^{15}N]nitrate molar ratio is about 1:1 at the beginning, unlike the endogenous nitrite and nitrate which occurred at a molar ratio of about 1:6. Also, plasma [^{15}N]nitrate concentration was relatively constant for about 3 h. These observations suggest that considerable amounts of administered S^{15}NACET or ^{15}NO-equivalents different from ALB-S^{15}NO are stored outside the plasma and are oxidized slowly to [^{15}N]nitrate.

Being an ester and electrically neutral at any pH value, SNACET is much better extractable into water-immiscible solvents such as ethyl acetate than the free acid SNAC, i.e., its product of enzymatic and non-enzymatic hydrolysis. We therefore undertook different measures to inhibit esterase-catalyzed hydrolysis of SNACET to SNAC and to stabilize the labile *S*-nitroso group against transition metal ions-catalyzed decomposition. Both the unselective esterase inhibitor PMSF and the chelator DTPA (Fig. 6) were found to be suitable in stabilizing SNACET in human plasma. In quantitative analyses we finally used DTPA alone. In the wider concentration range of 0–10 μM, SNACET (Fig. 7, Table 3) and all other tested LMM *S*-nitrosothiols were quantitated in plasma with analytically satisfactory recovery and precision. However, in the narrow concentration range of 0–1 μM, precision and linearity were acceptable, in contrast to recovery which was only of the order of 50% (Table 4). One reason for incomplete recovery may be that LMM *S*-nitrosothiols SNACET and GSNO were used as model *S*-nitrosothiols. Because of the commercial availability and ease synthesis and characterization as well as of the considerable stability of GSNO, this LMM *S*-nitrosothiol is widely used as a calibrator in almost all methods of *S*-nitrosothiol analysis [8,9,30,31]. Our results suggest that GSNO may be not useful for calibration purposes for other commonly analyzed HMM *S*-nitrosothiols, i.e., ALB-SNO and Hb-SNO, particularly because the plasma concentration of GSNO is presumably of the order of 1 nM and thus at least two orders of magnitude lower than of ALB-SNO [13,14]. Thus, use of *S*-nitrosothiols or structurally unrelated compounds [13] as internal standards or calibrators different from those finally analysed – a general practice in the area of *S*-nitrosothiols – seems to represent a major shortcoming in quantitative analyses of *S*-nitrosothiols and may lead to inaccurate results, even in MS-based methods in which stable-isotope labelled analogs may be used. This difficulty seems to be much less problematic in MS-based methods intended to measure a single *S*-nitrosothiol such as ALB-SNO or ^{15}N-labelled *S*-nitrosothiols [14,15].

By using the method reported here, we often observed for SNACET, both in distilled water and in plasma, differing regression equations between measured and added SNACET concentration by SIM of *m*/*z* 46 and *m*/*z* 47 on the one hand, and of *m*/*z* 157 and *m*/*z* 160 on the other hand. For instance, for SNACET extracted from dis-

tilled water we observed straight lines with almost the same slope values but different *y*-axis intercepts (Fig. 7A). On the other hand, for SNACET extracted from plasma converging straight lines were observed (Fig. 7B, C and D). In other words, detection of compound X (SIM of *m*/*z* 46 and *m*/*z* 47) may provide different SNACET concentrations than detection of compound Y (*m*/*z* 157 and *m*/*z* 160). The reasons for these observations are not completely understood. As distilled water and plasma do not contain SNACET, it is reasonable to assume that interfering species may also contribute to compound X. Indeed, we found that nitrite, which is ubiquitous and may be present in the ethyl acetate aliquot injected into the GC–MS apparatus, may also react in the hot injector with ethyl acetate to form compound X (Fig. 3), but not compound Y. An alternative explanation could be that the stoichiometry of the in-injector reaction of SNACET with ethyl acetate (Eq. (4)) changes, for unknown reasons, so that compound X is produced in excess of compound Y. Eventually, it may also be that reaction stoichiometry change and ethyl acetate contamination with nitrite occur simultaneously and contribute additively. The result of such a synergy would be diverging straight lines as illustrated in Fig. 7B, C and D.

$$\text{SNACET} + \text{ethyl acetate} \rightarrow \text{compound X} + \text{compound Y} \quad (4)$$

Because of unresolved methodological problems of the method described in the present work, we acknowledge that we cannot report on concrete numbers for basal levels for the sum of endogenous *S*-nitrosothiols in human plasma. Nevertheless, our study provides strong support that the concentration of *S*-nitrosothiols in plasma of healthy humans is clearly below about 500 nM. ALB-SNO is believed to be the most abundant endogenous *S*-nitrosothiol in human plasma. For this HMM *S*-nitrosothiol we determined previously by GC–MS basal plasma concentrations of the order of 160 nM [14,15]. Provided that ALB-SNO is indeed the most abundant *S*-nitrosothiol in human plasma, the concentration of LMM *S*-nitrosothiols including GSNO are at best in the lowest nM-range [8,9,13].

Thus far, only GSNO has been quantitated in human plasma by LC–MS/MS without any derivatization step but without the use of GS^{15}NO as internal standard [13]. It was reported that GSNO occurs in plasma of healthy humans at about 300 pM in basal conditions [13]. The procedures used in the present method in combination with the use of ^{15}N-labelled *S*-nitrosothiols as internal standards should be useful for the LC-ESI-MS/MS quantification of *S*-nitrosothiols in human plasma and other biological samples after their conversion to SNACET.

5. Conclusions

NACET is a useful reagent to convert in aqueous phase *S*-nitrosothiols into SNACET, which is quantitatively extracted into organic solvents such as chloroform and ethyl acetate. We discovered that injection of SNACET solutions in ethyl acetate, but not in chloroform, resulted in formation of two major GC peaks which were assigned to compound X and compound Y. The formation of these compounds was dependent upon the temperature of the injector. This in-injector reaction and the preceding *S*-transnitrosation reaction in aqueous phase were utilized to analyze various *S*-nitrosothiols in vitro and in vivo by the stable-isotope dilution GC–MS technique. Upon oral administration to rabbits, S^{15}NACET was not detectable in plasma unlike ALB-S^{15}NO, [^{15}N]nitrite and [^{15}N]nitrate which were identified as the major metabolites of S^{15}NACET. Ubiquitous nitrite was identified as interference in this method, too. Additional, not yet resolved methodological problems hampered accurate quantitative determination of the sum of *S*-nitrosothiols in human plasma. Nevertheless, the results of the present work together with previous findings from our group using a specific GC–MS method for ALB-SNO in human plasma and from the majority of other groups (discussed in Refs. [8,9]) suggest that the total concentration of *S*-nitrosothiols in plasma of healthy humans in the basal state is below 200 nM. Finally, this and a recent work from our group [35] underline the superiority of the use of stable-isotope labelled *S*-nitrosothiols and GC–MS to study in vitro and in vivo reactions and metabolism of *S*-nitrosothiols.

Acknowledgements

Andrzej Surdacki, current address Department of Cardiology, Jagiellonian University, 31-501 Cracow, Poland, was a recipient of the Humboldt research fellowship.

References

[1] P.C. Jocelyn, Biochemistry of the SH Group, Academic Press, 1972.
[2] T. Peters Jr., Adv. Protein Chem. 37 (1985) 161.
[3] J.S. Stamler, O. Jaraki, J. Osborne, D.I. Simon, J. Keaney, J. Vita, D. Singel, C.R. Valeri, J. Loscalzo, Proc. Natl. Acad. Sci. U.S.A. 89 (1992) 7674.
[4] T. Rassaf, N.S. Bryan, R.E. Maloney, V. Specian, M. Kelm, B. Kalyanaraman, J. Rodriguez, M. Feelisch, Nat. Med. 9 (2003) 481.
[5] A.N. Schechter, M.T. Gladwin, N. Engl. J. Med. 348 (2003) 1483.
[6] D. Giustarini, A. Milzani, R. Colombo, I. Dalle-Donne, R. Rossi, Trends Pharmacol. Sci. 25 (2004) 311.
[7] Y. Zhang, N. Hogg, Free Radic. Biol. Med. 38 (2005) 831.
[8] D. Giustarini, A. Milzani, I. Dalle-Donne, R. Rossi, J. Chromatogr. B 851 (2007) 124.
[9] D. Tsikas, Anal. Biochem. 379 (2008) 139.
[10] D. Tsikas, M. Ikic, K.S. Tewes, M. Raida, J.C. Frölich, FEBS Lett. 442 (1999) 162.
[11] D.J. Meyer, H. Kramer, N. Özer, B. Coles, B. Ketterer, FEBS Lett. 345 (1994) 177.
[12] D. Tsikas, J. Sandmann, S. Rossa, F.-M. Gutzki, J.C. Frölich, Anal. Biochem. 270 (1999) 231.
[13] D. Taubert, R. Roesen, C. Lehmann, N. Jung, E. Schömig, JAMA 298 (2007) 49.
[14] D. Tsikas, J. Sandmann, F.-M. Gutzki, D.O. Stichtenoth, J.C. Frölich, J. Chromatogr. B 726 (1999) 13.
[15] D. Tsikas, J. Sandmann, J.C. Frölich, J. Chromatogr. B 772 (2002) 335.
[16] D. Tsikas, J. Sandmann, S. Rossa, F.M. Gutzki, J.C. Frölich, Anal. Biochem. 272 (1999) 117.
[17] D. Tsikas, Curr. Pharm. Anal. 1 (2005) 15.
[18] H.M.H. van Eijk, Y.C. Luiking, N.E.P. Deutz, J. Chromatogr. B 851 (2007) 172.
[19] D. Tsikas, S. Rossa, D.O. Stichtenoth, M. Raida, F.M. Gutzki, J.C. Frölich, Biochem. Biophys. Res. Commun. 220 (1996) 939.
[20] D. Tsikas, J. Sandmann, S. Rossa, J.C. Frölich, J. Chromatogr. B 726 (1999) 1.
[21] D. Tsikas, M. Raida, J. Sandmann, S. Rossa, W.G. Forssmann, J.C. Frölich, J. Chromatogr. B 742 (2000) 99.
[22] D. Tsikas, Anal. Chem. 72 (2000) 4064.
[23] R. Rossi, D. Giustarini, A. Milzani, R. Colombo, I. Dalle-Donne, Circ. Res. 89 (2001) e47.
[24] D. Tsikas, J.C. Frölich, Circ. Res. 90 (2002) e39.
[25] D. Tsikas, Nitric Oxide 9 (2003) 53.
[26] J.S. Stamler, Circ. Res. 94 (2004) 414.
[27] D. Tsikas, Circ. Res. 94 (2004) e106.
[28] D. Tsikas, J.C. Frölich, Nitric Oxide 11 (2004) 209.
[29] D. Tsikas, in: I. Dalle-Donne, A. Scaloni, D.A. Butterfield (Eds.), Redox Proteomics: From Protein Modifications to Cellular Dysfunction and Diseases., John Wiley & Sons, Inc., Hoboken, 2006, p. p. 287.
[30] P.H. MacArthur, S. Shiva, M.T. Gladwin, J. Chromatogr. B 851 (2007) 93.
[31] A. Gow, A. Doctor, J. Mannick, B. Gaston, J. Chromatogr. B 851 (2007) 140.
[32] D. Tsikas, R. Rossi, JAMA 298 (2007) 1862, Reply: D. Taubert, N. Jung, R. Rosen, JAMA 298 (2007) 1863.
[33] R. Rossi, D. Tsikas, Clin. Chem. 55 (2009) 103, Reply: Y. Wu, W. Cha, F. Zhang, M.E. Meyerhoff, Clin. Chem. 55 (2009) 1039.
[34] G.A. Smythe, G. Matanovic, D. Yi, M.W. Duncan, Nitric Oxide 3 (1999) 67.
[35] A. Warnecke, P. Luessen, J. Sandmann, M. Ikic, S. Rossa, F.M. Gutzki, D.O. Stichtenoth, D. Tsikas, J. Chromatogr. B 877 (2009) 1375.